DEUTSCHES ELEKTRONEN – SYNCHROTRON DESY

DESY 86-163
December 1986

PHYSICS AT LEP

by

R.D. Peccei

Deutsches Elektronen-Synchrotron DESY, Hamburg

ISSN 0418-9833

NOTKESTRASSE 85 · 2 HAMBURG 52

To be sure that your preprints are promptly included in the
HIGH ENERGY PHYSICS INDEX,
send them to the following address (if possible by air mail):

DESY
Bibliothek
Notkestrasse 85
2 Hamburg 52
Germany

DESY 86-163
December 1986

ISSN 0418-9833

PHYSICS AT LEP

R.D Peccei

Deutsches Elektronen Synchrotron, DESY
Hamburg, Fed. Rep. Germany

Lectures presented at the 1986 CERN School of Physics, Sandhamn, Sweden, June 1986. Part of these lectures were also given at the XIV International Winter Meeting on Fundamental Physics, St. Feliu de Guixols, Spain, March 1986

PHYSICS AT LEP

R.D. Peccei
Deutsches Elektronen Synchrotron, DESY
Hamburg, Fed. Rep. of Germany

ABSTRACT

These lectures are devoted to a discussion of some of the physics which will be forthcoming from LEP. Among the topics discussed are electroweak physics at the Z^0 pole and above the W pair threshold, searches for Higgs bosons and for non standard physics phenomena at LEP.

PROLOGUE

The object of these lectures is to discuss some of the exciting physics which will be forthcoming at the new generation of e^+e^- colliders, SLC and LEP, operating in the 100 GEV range. I shall, for the most part, concentrate my discussion on electroweak physics, for two reasons. First and foremost, this physics is exceedingly interesting and is likely to be the focus of the experimental program at SLC and LEP. Secondly, deviations from the standard electroweak theory, although very important, are likely to be small. Thus it is well worthwhile to discuss in some detail the expectations of the standard model, including any possible inherent uncertainties.

Most of the material in these lectures is contained in one form or another in the recent report of the LEP Jamboree: Physics at LEP, edited by J. Ellis and R.D. Peccei, CERN Yellow Report CERN 86-02. I shall, in what follows, refer to material in this report simply as YR, indicating the volume and page number. I owe a debt of gratitude to all the participants in the working groups of the LEP Jamboree for their splendid efforts, which made the preparation of these lectures a relatively light task.

I. ELECTROWEAK PHYSICS AT THE Z^0 POLE

The principal concern of LEP 100 and of SLC will be to investigate electromagnetic and weak interactions in the vicinity of the Z^0 pole. To lowest order in the couplings of the electroweak standard model[1], the production of a fermion antifermion pair is given by the diagrams of Fig I.1

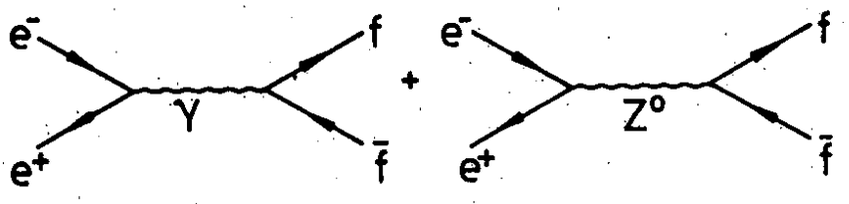

Fig I.1: Photon and Z^0 contributions to the process $e^+e^- \to f\bar{f}$

At $\sqrt{s} = M_Z$ the contribution of the second diagram above is of order

$$\sigma_{NC} \sim \frac{M_Z^2}{\Gamma_Z^2} \sigma_{em} \sim 10^3 \sigma_{em} \tag{I.1}$$

since

$$\sigma_{em}(e^+e^- \to \mu^+\mu^-) = \frac{4\pi\alpha^2}{3s} \simeq \frac{87 \text{ nb}}{(\sqrt{s}\text{GeV})^2} \simeq 10 \text{ pb} \Big|_{\sqrt{s}=M_Z} \tag{I.2}$$

one sees that at the Z^0 peak one expects a cross section of order:

$$\sigma_{Z_0 peak} \simeq 10 \text{ nb} \tag{I.3}$$

LEP 100 should operate with a luminosity near

$$\mathcal{L}_{LEP\ 100} \simeq 10^{31} \text{ cm}^{-2} \text{ sec}^{-1} \tag{I.4}$$

Thus in a year (of 10^7 sec) one should gather

$$\int \mathcal{L} dt \Big|_{year} \simeq 100 \text{ pb}^{-1} \tag{I.5}$$

of luminosity, which corresponds to 10^6 Z^0's. A somewhat smaller number of Z^0 per year is expected at the SLC. It is clear, at any rate, that with these many Z^0's, one should be able to perform precision tests of the standard electroweak theory.

Ia Z^0 WIDTH, $B(Z^0 \to f\bar{f})$ AND NEUTRINO COUNTING

In the standard SU(2)xU(1) model, the electroweak interactions of fermions are described by the following interaction Lagrangian:

$$\mathcal{L}_{int} = e J^\mu_{em} A_\mu + \frac{e}{2\sqrt{2}\sin\theta_W}(J^\mu_+ W_{-\mu} + J^\mu_- W_{+\mu}) + \frac{e}{2\cos\theta_W \sin\theta_W} J^\mu_{NC} Z_\mu \tag{I.6}$$

where the first term in the above describes the electromagnetic (em) interactions, the second the charged current (CC) interactions and the last the neutral current (NC) interactions. The currents characterizing these interactions in Eq(I.6) have different Lorentz transformation properties. The electromagnetic current

$$J^\mu_{em} = \sum_f e_f \bar{f}\gamma^\mu f \tag{I.7}$$

with

$$e_f = \begin{cases} -1 & \text{charged leptons} \\ +2/3 & \text{u-like quarks} \\ -1/3 & \text{d-like quarks} \end{cases} \qquad (I.8)$$

is a purely vector current. The charged currents

$$J^{\mu}_{+} = (\bar{\nu}_e \bar{\nu}_\mu \bar{\nu}_\tau)\gamma^{\mu}(1-\gamma_5)1 \begin{pmatrix} e \\ \mu \\ \tau \end{pmatrix} + (\bar{u}\bar{c}\bar{t})\gamma^{\mu}(1-\gamma_5)V_{KM} \begin{pmatrix} d \\ s \\ b \end{pmatrix} \qquad (I.9a)$$

$$J^{\mu}_{-} = (J^{\mu}_{+})^{+} \qquad (I.9b)$$

where V_{KM} is the Cabibbo-Kobayashi-Maskawa[2] mixing matrix, on the other hand, have a V-A structure, reflecting the fact that only the left handed fermions have non trivial transformation properties under SU(2). Finally, the neutral current

$$J^{\mu}_{NC} = 2(J^{\mu}_{3} - \sin^2\theta_W J^{\mu}_{em}) \qquad (I.10)$$

has mixed vector and axial vector transformation properties, as one can see from its definition. Explicitly, one can write Eq(I.10) as

$$J^{\mu}_{NC} = 2 \Sigma \bar{f} (V_f \gamma^{\mu} + A_f \gamma^{\mu}\gamma_5) f \qquad (I.11)$$

and one finds for the constants V_f and A_f:

$$V_f = \frac{1}{2} (T_3)_f - e_f \sin^2\theta_W \qquad (I.12)$$

$$A_f = -\frac{1}{2} (T_3)_f$$

where

$$(T_3)_f = \begin{cases} +1/2 & \text{neutrinos, u-like quarks} \\ -1/2 & \text{charged leptons, d-like quarks} \end{cases} \qquad (I.13)$$

Using Eq(I.6) and the explicit form for J^{μ}_{NC}, it is straightforward to compute the Z^0 partial width into fermion-antifermion pairs. The decay amplitude is given by

$$T = \frac{e}{\cos\theta_W \sin\theta_W} \epsilon^{\mu}_{Z}(\lambda)\, \bar{u}_f(p_f, s_f) [\gamma_\mu V_f + \gamma_\mu \gamma_5 A_f] v_{\bar{f}}(p_{\bar{f}}, s_{\bar{f}}) \qquad (I.14)$$

so that the decay width of an unpolarized Z^0, at rest, into a fermion-antifermion pair, whose polarizations are not detected, is given by

$$\Gamma(Z^0 \to f\bar{f}) = \frac{1}{2M_Z} \int \frac{d^3p_f}{(2\pi)^3 2E_f} \frac{d^3p_{\bar{f}}}{(2\pi)^3 2E_{\bar{f}}} (2\pi)^4 \delta^4(p_Z - p_f - p_{\bar{f}}) \cdot \frac{1}{3} \sum_{\lambda} \sum_{s_f s_{\bar{f}}} |T|^2 \qquad (I.15)$$

It is easy to check that there is no $V_f - A_f$ interference in Eq(I.15). Furthermore, if one neglects the mass of the produced fermions, then V_f and A_f contribute the same to the partial width. A straightforward calculation gives the result:

$$\Gamma(Z^0 \to f\bar{f}) = \frac{e^2 M_Z}{12\pi \sin^2\theta_W \cos^2\theta_W} c_f (V_f^2 + A_f^2)$$

$$= \frac{\sqrt{2}\, G_F\, M_Z^3}{3\pi} c_f (V_f^2 + A_f^2) \qquad (I.16)$$

In the above c_f is a color factor:

$$c_f = \begin{cases} 1 & \text{leptons} \\ 3 & \text{quarks} \end{cases} \qquad (I.17)$$

The second line in Eq(I.16) follows by using the tree level SU(2)xU(1) relation for the Fermi constant

$$\frac{G_F}{\sqrt{2}} = \frac{e^2}{8\sin^2\theta_W M_W^2} \qquad (I.18)$$

along with the relation between M_W and M_Z, which follows if the breakdown of SU(2)xU(1) to $U(1)_{em}$ is accomplished by a doublet of Higgs:

$$M_W^2 = M_Z^2 \cos^2\theta_W \qquad (I.19)$$

As I will discuss in detail later, radiative corrections alter the expressions (I.16) for $\Gamma(Z^0 \to f\bar{f})$. It turns out, however, that using the second expression in Eq(I.16) these corrections are very small, and for all practical purposes can be neglected.

Using Eq(I.16), the relative rates for the various Z^0 decay channels are easily determined. One finds:

$$\Gamma(Z^0 \to \nu_e \bar{\nu}_e) = (1 + 1)\Gamma_0 = 2\Gamma_0 \qquad (I.20a)$$

$$\Gamma(Z^0 \to e^- e^+) = (1 + (1 - 4\sin^2\theta_W)^2)\Gamma_0 \simeq 1.01\ \Gamma_0 \qquad (I.20b)$$

$$\Gamma(Z^0 \to u\bar{u}) = 3(1 + (1 - \tfrac{8}{3}\sin^2\theta_W)^2)\Gamma_0 \simeq 3.45\ \Gamma_0 \qquad (I.20c)$$

$$\Gamma(Z^0 \to d\bar{d}) = 3(1 + (1 - \tfrac{4}{3}\sin^2\theta_W)^2)\Gamma_0 \simeq 4.44\ \Gamma_0 \qquad (I.20d)$$

The numerical results in the above use $\sin^2\theta_W = 0.23$. The constant Γ_0 in these equations is given by

$$\Gamma_0 = \frac{G_F M_Z^3}{24\sqrt{2}\,\pi} \approx 85 \text{ MeV} \tag{I.21}$$

where the numerical result applies for $M_Z = 92$ GeV. Thus, for the leptons, one expects the partial rates

$$\Gamma(Z^0 \to \nu_e \bar{\nu}_e) \approx 170 \text{ MeV} \tag{I.22}$$

$$\Gamma(Z^0 \to e^- e^+) \approx 86 \text{ MeV} \tag{I.23}$$

The quark partial rates are slightly increased from the values given in Eq(I.20) by QCD effects. Since quarks carry color, in the Z^0 decay process into quarks one must also take into account the possibility of having both virtual and real gluons, as shown in Fig I.2.

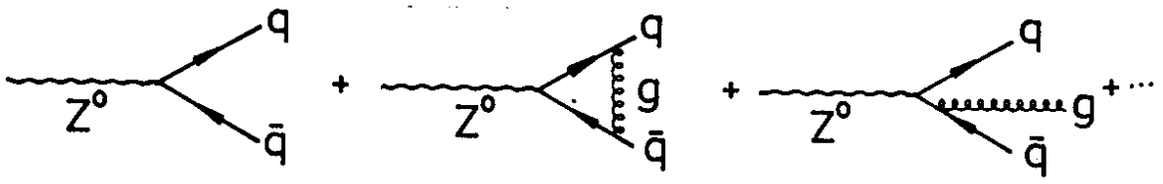

Fig. I.2: QCD corrections to the decay process $Z^0 \to q\bar{q}$

To lowest order in α_s, the effect of QCD is to multiply the rate for quarks by a factor of $1 + \alpha_s/\pi$. Not surprisingly, this factor is identical to that for the total e^+e^- cross section[3], since, neglecting the quark masses, the QCD corrections to the vector and axial vector vertex are the same. QCD corrections, therefore, amount to a redefinition of the color factor c_f in Eq(I.17):

$$c_f = \begin{cases} 1 & \text{leptons} \\ 3\left[1 + \frac{\alpha_s}{\pi}(M_Z) + \ldots\right] & \text{quarks} \end{cases} \tag{I.24}$$

Using the estimate[4]

$$\frac{\alpha_s}{\pi}(M_Z) = 0.04 \pm 0.01 \tag{I.25}$$

gives for the Z^0 partial rates into $u\bar{u}$ and $d\bar{d}$ the numerical values ($M_Z = 92$ GeV; $\sin^2\theta_W = 0.23$)

$$\Gamma(Z^0 \to u\bar{u}) \approx 306 \text{ MeV} \tag{I.26}$$

$$\Gamma(Z^0 \to d\bar{d}) \approx 393 \text{ MeV} \tag{I.27}$$

For three families of quarks and leptons, summing up all the partial rates except for that of $Z^0 \to t\bar{t}$, gives for the total width the value

$$\Gamma(Z^0 \to \text{all})\Big|_{\text{no top}} = (2560 \pm 20)\ \text{MeV} \qquad (I.28)$$

The above uses the assumed values for M_Z and $\sin^2\theta_W$. The error shown is due to the uncertainty in α_s. Since the top quark mass is still unknown (the UA1 collaboration reported preliminary indications[5] for a top mass in the 30-50 GeV range, but these indications have not been confirmed), it is not clear whether the decay $Z^0 \to t\bar{t}$ will be kinematically allowed. If $Z^0 \to t\bar{t}$ is in fact an allowed decay, it is clear that the partial width will be quite sensitive to the precise value of m_t. The top quark mass enters kinematically in the expression for the partial width through the appearance of β factors due to the more limited phase space, where as usual

$$\beta = (1 - 4\, m_t^2/M_Z^2)^{1/2} \qquad (I.29)$$

Furthermore, for small β the QCD corrections to the rate are enhanced[6] and differ for the vector and axial vector contributions. Including the kinematical effects of a nonvanishing top mass and $O(\alpha_s)$ QCD corrections[6] one finds

$$\Gamma(Z^0 \to t\bar{t}) = \frac{\sqrt{2}\, G_F\, M_Z^3}{\pi} \left[V_t^2\, \beta\, \frac{(3 - \beta^2)}{2}\, X_V + A_t^2\, \beta^3\, X_A \right] \qquad (I.30)$$

Here X_V and X_A are QCD correction factors, which read:

$$X_V = 1 + \frac{\alpha_s}{\pi} + \frac{2\pi}{3}\,\alpha_s \left(\frac{1}{\beta} - \frac{(3 + \beta)}{4} \right) \qquad (I.31a)$$

$$X_A = 1 + \frac{\alpha_s}{\pi} + \frac{2\pi}{3}\,\alpha_s \left(\frac{1}{\beta} - \left(\frac{19}{10} - \frac{22}{5}\,\beta + \frac{7}{2}\,\beta^2 \right) \right) \qquad (I.31b)$$

Although the terms in the curly brackets in Eqs(I.31) vanish as $\beta \to 1$, for heavy top quarks they become very large due to the $1/\beta$ factors. For example for $m_t = 40$ GeV then $\beta \approx 1/2$ and one has as QCD correction factors

$$X_V \approx 1.34 \quad ; \quad X_A \approx 1.42 \qquad (I.30)$$

instead of the naive expectation $X_V = X_A = (1 + \frac{\alpha_s}{\pi}) \approx 1.04$. The QCD corrected rate for $m_t = 40$ GeV is

$$\Gamma(Z^0 \to t\bar{t}) \approx 81\ \text{MeV} \qquad (I.31)$$

Fig I.3 shows this rate, normalized by the rate into $\mu^+\mu^-$ pairs, as a function of m_t

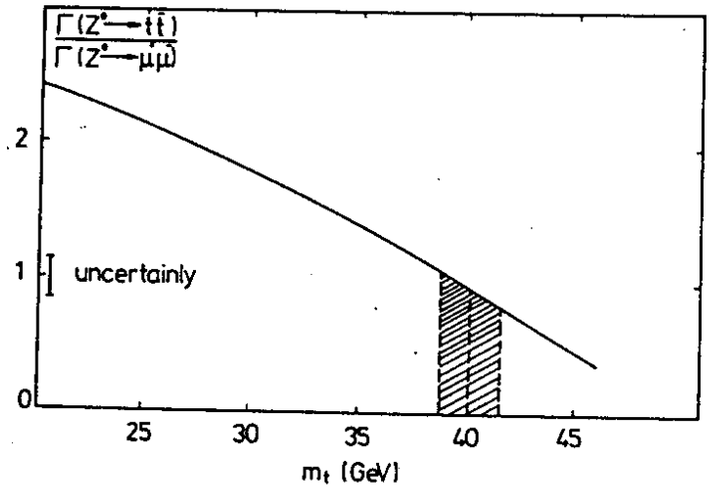

Fig I.3: Decay rate of $Z^0 \to t\bar{t}$ normalized to that for $Z^0 \to \mu^+\mu^-$

Because for m_t near $\frac{1}{2} M_Z$ the QCD corrections are large, it is natural to worry about higher order terms. The appearance of the α_s/β terms in Eqs(I.31) are particularly troubling but, fortunately, the origin of these contributions and how one can handle them is well known[7]. Terms of $O((\alpha_s/\beta)^n$ are due to the exchange of n soft Coulomb gluons. However, since the precise form of the Coulomb wave function is known, all these contributions can be summed up exactly[8]. This summation corresponds to making the following effective replacement in Eq(I.31):

$$1 + \frac{2\pi\alpha_s}{3\beta} \to \frac{\frac{4\pi\alpha_s}{3\beta}}{[1 - e^{-\frac{4\pi\alpha_s}{3\beta}}]} \qquad (I.32)$$

Note that using (I.32) it appears that one still obtains a finite rate in (I.30) in the $\beta \to 0$ limit! In fact, this perturbative treatment stops being valid long before that. For $\beta \sim \alpha_s$ one must begin to worry also about the quarkonia bound states which the multiple exchange of soft gluons will form. I shall not discuss here further the effects of toponium-Z^0 mixing, but refer the interested reader to the papers of Ref 9. I just note that for m_t = 40 GeV the effect of the resumation in (I.32) is not dramatic. It corresponds to the replacement: 1.53 → 1.62, so that the rate plotted in Fig I.3 is probably underestimated by 6% at this value of m_t.

At any rate, the principal uncertainty in the rate for $Z^0 \to t\bar{t}$ is not really theoretical but due to our lack of knowledge of the actual value for m_t. Indeed, to get a precise value for the total width for the Z^0, predicted by the standard model for 3 generations, one will need to know m_t as well as possible. Buchmüller et al[10] have studied this issue in some detail and have suggested two ways of arriving at an accurate value for m_t. These are:

i) Isolate the $t\bar{t}$ decays of the Z^0 topologically. This should be possible since these decays lead typically to multijets in the final state. Once the branching ratio $\Gamma(Z^0 \to t\bar{t})/\Gamma(Z^0 \to \mu^-\mu^+)$ is established, then a value of m_t follows from the theoretically predicted ratio of Fig I.3.

ii) More directly, once a certain fraction of t-decays are identified, then m_t can be extracted from a measurement of the multijet invariant mass distribution.

Buchmüller et al[10] conclude that one can hope to pin down m_t to within a GeV. Being a bit more conservative, it is probably reasonable to expect that m_t will be known to $\delta m_t = \pm$ 2GeV. From Fig I.3, for m_t near 40 GeV, this uncertainty translates in an error for the partial width

$$\delta\Gamma(Z^0 \to t\bar{t}) \simeq 30 \text{ MeV} \tag{I.33}$$

Hence, the prediction for the total Z^0 width for m_t = 40 GeV, M_Z = 92 GeV and $\sin^2\theta_W$ = 0.23 is

$$\Gamma(Z^0 \to \text{all}) = (2641 \pm 20 + 30) \text{ MeV} \tag{I.34}$$

where the first error is due to the α_s uncertainty and the other to δm_t.

The actual prediction for $\Gamma(Z^0 \to \text{all})$, once M_Z and $\sin^2\theta_W$ are measured with accuracy, might have a slightly different numerical value than (I.34), depending on the central values of these parameters. It also will have a somewhat larger error estimate, because both $\sin^2\theta_W$ and M_Z have associated measurement errors. For 3 generations and neglecting t quark mass effects one has

$$\delta\Gamma(Z^0 \to \text{all}) = 96\Gamma_0(1 - \frac{8}{3}\sin^2\theta_W)\delta\sin^2\theta_W \tag{I.35}$$

As I shall discuss later on, an error on $\sin^2\theta_W$ of $\delta\sin^2\theta_W \leq 0.004$ should certainly be achievable at LEP 100, which implies using (I.35) an uncertainty in the total width

$$\delta\Gamma(Z^0 \to \text{all}) \Big|_{\delta\sin^2\theta_W} \simeq 10 \text{ MeV} \tag{I.36}$$

An uncertainty in the Z^0 mass itself of 50 MeV - a number which, as I will discuss, is achievable at LEP 100 - gives a further uncertainty in $\Gamma(Z^0 \to \text{all})$ of:

$$\delta\Gamma(Z^0 \to \text{all}) \Big|_{\delta M_Z^0} = 3\Gamma(Z^0 \to \text{all}) \frac{\delta M_Z}{M_Z} \simeq 4 \text{ MeV} \tag{I.37}$$

Finally, one has to worry about the electroweak radiative corrections to the theoretical formulas we have used to compute $\Gamma(Z^0 \to \text{all})$. For reasons which I will discuss later in some detail, it turns out that the total width defined through the formula

$$\Gamma(Z^0 \to \text{all}) = 16\Gamma_0 \sum_f c_f(V_f^2 + A_f^2) \tag{I.38}$$

has very small radiative corrections, provided that $\sin^2\theta_W$ is defined also to $O(\alpha)$ by the ratio of the W and Z^0 masses:

$$\sin^2\theta_W = 1 - \frac{M_W^2}{M_Z^2} \qquad (I.39)$$

Typically one finds[11]

$$\delta\Gamma_{Rad} \simeq (1 - 2)\times 10^{-3}\ \Gamma(Z^0 \to \text{all}) \simeq (3 - 6)\text{MeV} \qquad (I.40)$$

where the precise value depends on the detailed values for M_Z and $\sin^2\theta_W$.

Putting all these numbers together, the expectation for the total width, including radiative corrections, for M_Z = 92 GeV, $\sin^2\theta_W$ = 0.23, m_t = 40 GeV is

$$\Gamma(Z^0 \to \text{all}) = (2645 \pm 20 \pm 30 \pm 10 \pm 4)\text{MeV} \qquad (I.41)$$

where the errors shown are our estimates for uncertainties in α_s, m_t, $\sin^2\theta_W$ and M_Z, respectively. It is possible that all these errors can be reduced internally in each experiment. For instance, QCD studies can give a better determination of $\alpha_s(M_W)$; toponium physics can probably pin down m_t to better than 2 GeV; precise electroweak measurements can reduce the uncertainty in $\sin^2\theta_W$. Since the errors in (I.41) seem, at any rate, to be rather small, it is clear that if a precise measurement of $\Gamma(Z^0 \to \text{all})$ is feasible at LEP 100, then one should be able to put a strong bound on possible unseen modes. For instance, an extra neutrino generation would provide an additional width contribution of 170 MeV, which is much above the errors in (I.41).

Considerable energy has been expended to see what is the intrinsic width accuracy for the Z^0 that one can hope to obtain at LEP 100. This analysis is not trivial in that radiative effects substantially alter the naive expectations. Only after these radiative effects are accounted for, can one hope to extract a Z^0 width suitable for comparison with the theoretical formulas discussed above. Let me try to explain this point with some care. Experimentally, the most straightforward way to measure the total Z^0 width is by studying the process $e^+e^- \to \mu^+\mu^-$, in the vicinity of the Z^0 resonance. The total cross section for this process to lowest order in α, is easily computed from the graphs of Fig I.4.

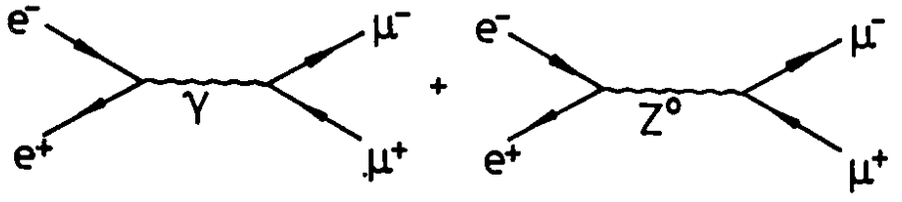

Fig I.4 Graphs contributing to $e^+e^- \to \mu^+\mu^-$

The effect of the Z^0 width is incorporated explicitly in the Z^0 propagator by the replacement

$$\frac{1}{s - M_Z^2} \rightarrow \frac{1}{s - M_Z^2 + iM_Z\Gamma_{tot}} \qquad (I.42)$$

A straightforward calculation, dropping fermion mass terms, gives the formula

$$\sigma(e^+e^- \rightarrow \mu^+\mu^-) = \frac{4\pi\alpha^2}{3s}\left\{1 + \frac{2s(s - M_Z^2)}{\sin^2\theta_W \cos^2\theta_W}\,\frac{V_e^2}{|s - M_Z^2 + iM_Z\Gamma_{tot}|^2}\right.$$

$$\left. + \frac{s^2}{\sin^4\theta_W\cos^4\theta_W}\,\frac{(V_e^2 + A_e^2)^2}{|s - M_Z^2 + iM_Z\Gamma_{tot}|^2}\right\} \qquad (I.43)$$

The general structure of this formula is easy to understand. As was the case for the Z^0 width, also here there are no V-A interference terms. This means that the γ-Z cross term must be proportional to $(1.V_e)\times(1.V_\mu) \equiv V_e^2$, while the Z^2 term must have the structure $(V_e^2+A_e^2)\times(V_\mu^2+A_\mu^2) \equiv (V_e^2+A_e^2)^2$, as is explicitly apparent from (I.43). Further the cross section, because of the substitution (I.42), has the characteristic Breit-Wigner line shape, which is symmetric about $\sqrt{s} = M_Z$. A measurement of this line shape then should give Γ_{tot} directly.

This naive expectation, however, is not fullfilled in practice, since QED radiative effects substantially alter the line shape. The principal modifications arise because of initial state radiation from the incident $e^+$and e^- beams (see Fig I.5).

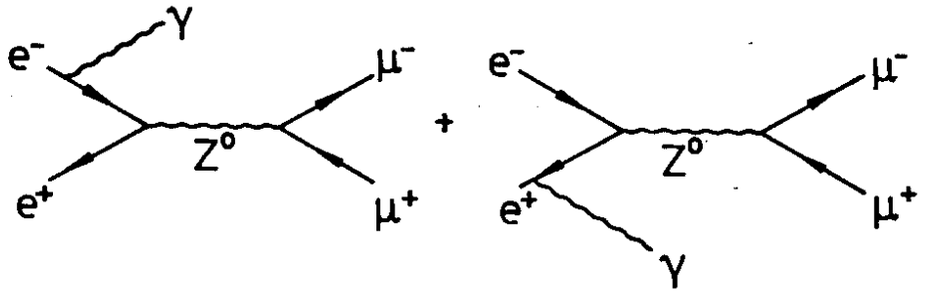

Fig I.5 Initial state radiation, giving rise to line shape modifications

It is easy to understand kinematically that the effect of this initial state radiations is to:

i) shift the peak for the process $e^+e^- \rightarrow \mu^+\mu^-$ above $\sqrt{s} = M_Z$

ii) give rise to a long radiative tail for $\sqrt{s} > M_Z$.

Both these phenomena are illustrated in Fig I.6, where the lowest order cross section is contrasted with what is expected once one includes first order QED corrections, for a reasonable set of experimental cuts

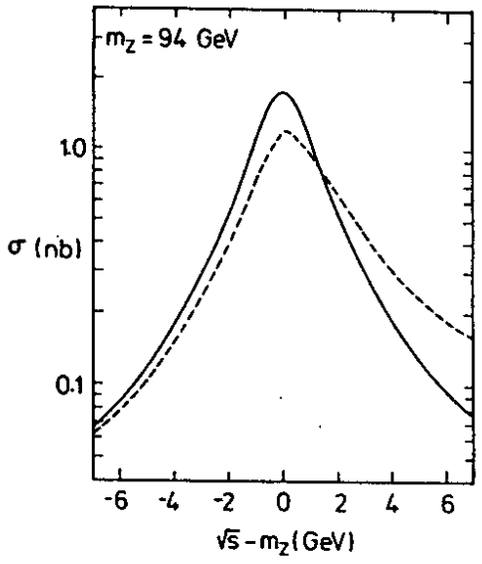

Fig I.6 Total cross section for the process $e^+e^- \to \mu^+\mu^-(\gamma)$ in lowest order (solid line) and QED corrected (dashed line), from Ref 12). The parameters and cuts used here are: M_Z = 94 GeV, Γ_Z = 2.67 GeV, $\sin^2\theta_W$ = 0.2157 and E_{μ^+}, $E_{\mu^-} > 10$ GeV, $5^0 < \theta_{\mu e} < 175^0$, $\xi_{acol} = 10^0$.

The size of these effects can be estimated roughly to give a mass shift δM_Z and an increase in the width $\delta\Gamma_Z$ of order [4]

$$\delta M_Z^{em} \sim \delta\Gamma_Z^{em} \sim \frac{\alpha}{\pi} \ln \frac{M_Z^2}{m_e^2} \Gamma_{tot} \sim 150 \text{ MeV} \qquad (I.44)$$

Thus these effects are far from negligible and one will have to unfold them to extract accurate values for Γ_{tot} and M_Z.

Using the QED corrected line shape, however, it is expected that the actual experimental error incurred for Γ_{tot} will be much smaller than $\delta\Gamma_Z^{em}$. This issue has been studied by Blondel et al[13] who suggested performing a scan from $\sqrt{s}$ = 80 GeV to $\sqrt{s}$ = 104 GeV with a 2 GeV step interval. Assuming that one can collect 2 pb^{-1} integrated luminosity per point, one would have approximately 4500 $\mu^+\mu^-$ pairs, of which 2000 in the peak, after the scan. This procedure, which should take from one to three months running time at LEP 100, should give a statistical error on Γ_{tot} of[13]

$$\delta\Gamma_{tot}^{stat} \lesssim 15 \text{ MeV} \qquad (I.45)$$

Blondel et al[13] also estimate that possible quadratic distorsions in the machine luminosity versus energy - distorsions which would lead to a change in the $e^+e^- \to \mu^+\mu^-$ profile - could give rise to a systematic uncertainty of order

$$\delta\Gamma_{tot}^{syst} \lesssim 10 \text{ MeV} \qquad (I.46)$$

If indeed the experimental accuracy achieved at LEP 100 is of the magnitude estimated above, it will be more than adequate to test the prediction of the standard model for Γ_{tot}, given in Eq I.41. Thus LEP 100 should be able to determine whether there are additional neutrinos, or other light neutral excitations which couple to the Z^0, beyond those of the known three generations. Although I am not aware of a similar detailed study for the SLC, it is expected that a comparable accuracy for Γ_{tot} will also be achievable there.

The above method to "count" extra neutrinos, or light excitations coupled to the Z^0, is rather indirect. There is an alternate, and more direct, way to do this neutrino counting, which uses the process $e^+e^- \to \gamma$ Nothing[14]. Here "Nothing" stands for any kind of neutral penetrating excitation and it includes, in particular, neutrino pairs. Near the Z^0 resonance this process gets dominant contributions from neutral excitations produced by virtual Z^0's. This is illustrated, for the particular case of neutrinos, by Fig I.7

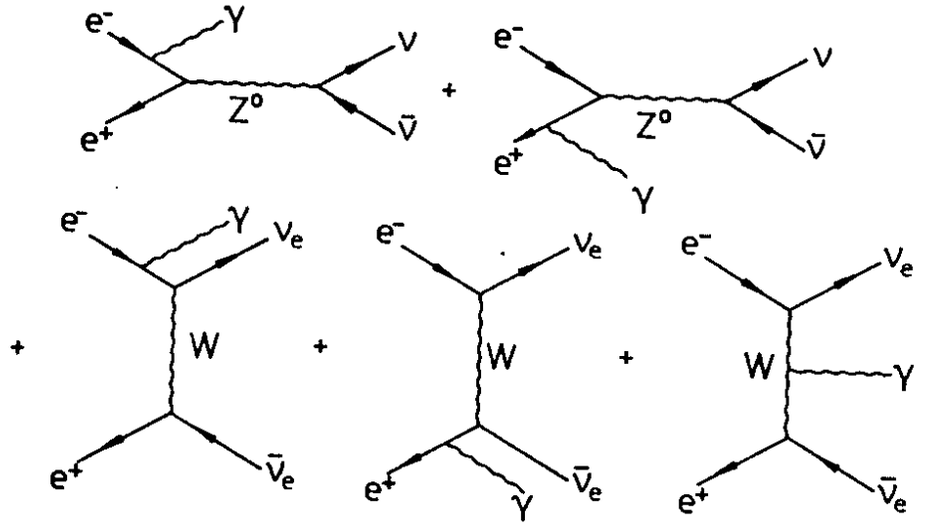

Fig I.7: Graphs contributing to the process $e^+e^- \to \nu\bar{\nu}\gamma$

The size of the cross section depends directly on the partial width of the Z^0 into neutral unseen excitations and so a measurement of $e^+e^- \to \gamma$ Nothing, in the vicinity of $\sqrt{s} = M_Z$, serves as a measure of this width.

To be specific, I will imagine that the only extra excitations coupled to the Z^0 are neutrinos from yet unseen generations. Then the cross section for the process $e^+e^- \to \gamma\nu\bar{\nu}$ can be computed directly from the graphs shown in Fig I.7. Note that if the pair of produced neutrinos are the electron neutrinos, then in addition to the dominant neutral current graphs involving Z^0 exchange, one must include also the charged current graphs. Of course, for the physically measurable process $e^+e^- \to \gamma$ Nothing one must sum over all neutrino species. I quote below the differential cross section for the process $e^+e^- \to \gamma$ Nothing, with Nothing being neutrinos, computed some time ago by Gaemers, Gastmans and Renard[15].

$$\frac{d\sigma}{dxdy} = \frac{\alpha G_F^2 s(1-x)}{3\pi^2 x(1-y^2)} \left[(1 - \tfrac{1}{2}x)^2 + \tfrac{1}{4} x^2 y^2 \right] F(x)$$

where

$$F(x) = 1 + \frac{2M_Z^2(M_Z^2 - s(1-x))(V_e - A_e) + 2M_Z^4 N_\nu (V_e^2 + A_e^2)}{[M_Z^2 - s(1-x)]^2 + M_Z^2 \Gamma_Z^2} \qquad (I.48)$$

In the above the parameters x and y are related to the photon energy and its angle, θ_γ, relative to the incoming e^- direction:

$$x = \frac{2E_\gamma}{\sqrt{s}} \qquad y = \cos\theta_\gamma \qquad (I.49)$$

while N_ν is the total number of neutrino species.

There are a number of observations that can be made about this differential cross section:

i) The three factors appearing in F(x) correspond to the pure W exchange contribution, the interference between the W exchange and the Z^0 exchange contributions and the pure Z^0 contributions, respectively. The first two of these terms occur only because of the presence of the $e^+e^- \to \nu_e\bar{\nu}_e\gamma$ process. Thus it is only the last term in F(x) which really counts the number of neutrinos.

ii) The relative magnitude between the terms appearing in (I.48) can be easily deduced by considering the limit when M_W and M_Z become large. In this limit, it is well known that the effective Lagrangian for $e^+e^- \to \nu_e\bar{\nu}_e$ due to W exchange can be Fierz transformed into a form involving only neutral currents. That is

$$\mathcal{L}_{eff}^{CC} = \frac{G_F}{\sqrt{2}} \bar{\nu}_e \gamma^\mu (1 - \gamma_5) e \; \bar{e} \gamma_\mu (1 - \gamma_5) \nu_e \qquad (I.50)$$

$$= \frac{G_F}{\sqrt{2}} \bar{\nu}_e \gamma^\mu (1 - \gamma_5) \nu_e \; \bar{e} \gamma_\mu (1 - \gamma_5) e$$

This means that the W exchange contribution can be incorporated simply by changing the constants V_e and A_e for electrons in the neutral current of Eq(I.11) to:

$$V_e^{eff} = V_e + \frac{1}{2} \qquad A_e^{eff} = A_e - \frac{1}{2} \qquad (I.51)$$

Thus in the heavy intermediate boson mass limit one would expect F(x) to reduce to

$$F(x) \to 2 \left\{ (N_\nu - 1)(V_e^2 + A_e^2) + ((V_e^{eff})^2 + (A_e^{eff})^2) \right\}$$

$$= 2N_\nu(V_e^2 + A_e^2) + 2(V_e - A_e) + 1 \qquad (I.52)$$

which is indeed the result obtained in this limit from (I.48)

iii) The cross section away from the neighborhood of the Z^0 resonance is of $O(\alpha G_F^2 s)$, as can be expected. Furthermore, the behaviour of the photon spectrum has the characteristic x^{-1} form. For energies close to the Z^0 mass the terms involving the Z^0 propagator, and therefore involving the number of neutrinos, are very much enhanced in F(x). This enhancement peaks at $x = 1 - M_Z^2/s$, which corresponds to

$$E_\gamma = \frac{\sqrt{s}}{2}\left(1 - \frac{M_Z^2}{s}\right) \approx \sqrt{s} - M_Z \qquad (I.53)$$

where the second expression follows only for $\sqrt{s}$ near M_Z.

The differential cross section for the process $e^+e^- \to \gamma$ Nothing, for the case in which Nothing is just the contribution of the neutrinos of 3 generations (therefore $N_\nu = 3$) is plotted in Fig I.8. In this figure, the dependence on $\cos\theta_\gamma$ has been integrated over, for photon angles lying in the interval $20^0 < \theta_\gamma < 160^0$. This angular cut, as I will discuss below, is done to suppress background. One sees that, as one increases the center of mass energy $\sqrt{s}$, the peak in the photon spectrum shifts, as predicted by Eq(I.53). The height of the peak is proportional to N_ν, which for this figure is taken as 3. Note also that the cross section decreases as E_γ increases, due to the 1/x factor in Eq(I.47).

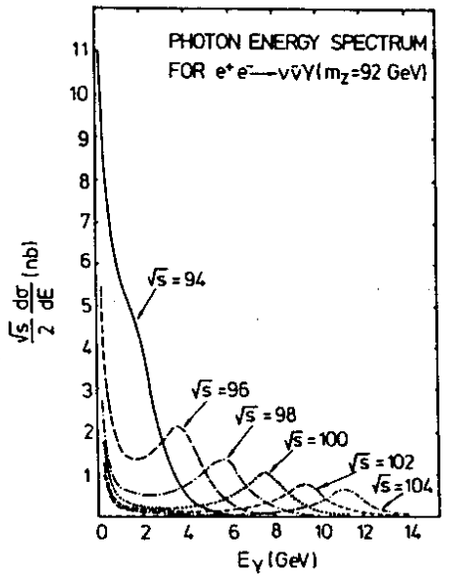

Fig I.8: Cross section for $e^+e^- \to \gamma$ Nothing for $N_\nu = 3$ integrated over all photon angles in the range $20^0 < \theta_\gamma < 160^0$. From Ref 16

Whether one can count the number of neutrinos this way at LEP depends mostly on how successful one is in suppressing the normal QED background from the process $e^+e^- \to e^+e^-\gamma$, in which both final charged particles are lost in the beam pipe. At LEP an electron is lost if $\theta_e \lesssim 6^0$ or $\theta_e \gtrsim 174^0$. Since photons produced at large θ_γ with respect to the beam axis, in general, do not arise from configurations with forward going electrons or positrons, the cut

$20^0 < \theta_\gamma < 160^0$ should substantially reduce the dangerous QED background. In her analysis in the Yellow report, Simopoulou[16] considered that this cut would suffice to remove most of the QED radiative Bhabha background, if one ran at energies a few GeV above the Z^0 resonance peak. However, her estimate of the background neglected certain kinematical configurations (forward going e^-, with θ_γ large) for which her numerical integration program became unstable. This problem has been reanalyzed recently by Caffo, Gatto and Remiddi[17] who find a much larger background than previously estimated, especially for relatively low photon energies. This is illustrated, for instance, in Fig I.9 where the signal expected for $N_\nu = 3$, for a cut of $25^0 < \theta_\gamma < 155^0$, is compared to the background calculation of Caffo, Gatto and Remiddi[17], for a center of mass energy about 5 GeV above the Z^0 mass.

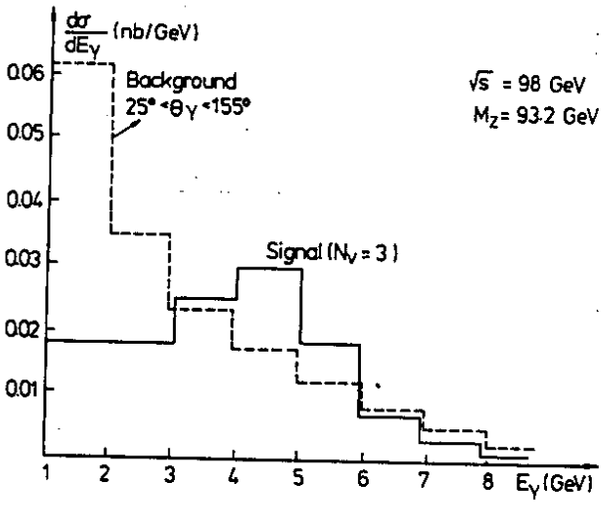

Fig I.9 Signal and background for a neutrino counting experiment with $25^0 < \theta_\gamma < 155^0$ and $\sqrt{s} - M_Z \approx 5$ GeV, from Ref 17

The estimate of Ref 16, for a similar experimental situation, would have given essentially a negligible background. An independent calculation by Maña and Martinez[18], which treated the sensitive numerical integration region in a different way than that of Ref 17, appears to give very similar results to those of Caffo, Gatto and Remiddi[17].

In view of the rather large background found, Caffo, Gatto and Remiddi[17] suggest that it may be sensible to try to do the neutrino counting experiment at energies only slightly above the Z^0 mass. Here the cross section, as can be seen from Fig I.8, is rather large and, if an accurate background subtraction can be performed, one may in the end be better off. This same point was made sometime ago by Bartels, Fridman, Wu and Schwarz[19]. An alternative possibility, however, is to run at energies much above the Z^0 mass where, even though the cross section is smaller, the background is really rather negligible. This is illustrated in Fig I.10.

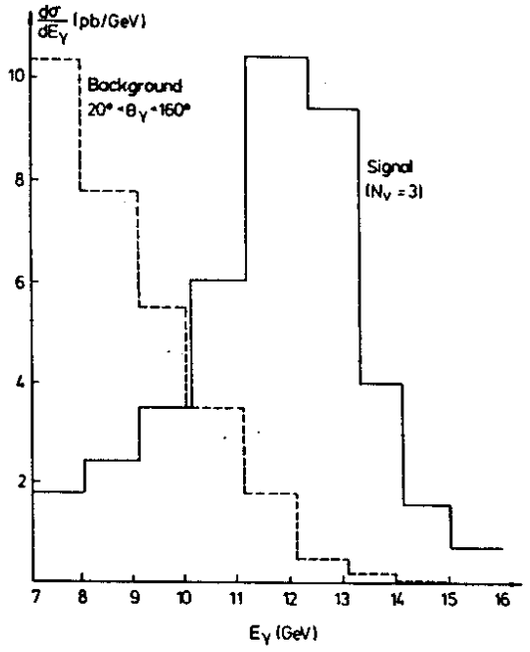

Fig I.10 Signal and background for a neutrino counting experiment with $20^0 < \theta_\gamma < 160^0$ and $\sqrt{s} - M_Z \simeq 13$ GeV

A dedicated run at $\sqrt{s} \simeq 106$ GeV with an integrated luminosity of 5 pb^{-1}, with a cut in θ_γ as indicated in Fig I.10, would produce 150 events with $E_\gamma > 10$ GeV, if $N_\nu = 3$, but 200 such events, if $N_\nu = 4$. Since the background is small, the change between $N_\nu = 3$ and $N_\nu = 4$ gives a 4σ effect.

As a last topic in this section, let me briefly discuss the Z^0 leptonic widths. These widths can be studied at LEP 100 directly by measuring the integral over the Z^0 resonance. In the vicinity of the resonance we can drop the photon contributions in Eq(I.43) and so this cross section takes a standard Breit Wigner form

$$\sigma(e^+e^- \to \mu^+\mu^-) = 12\pi \frac{\Gamma(Z^0\to e^+e^-)\Gamma(Z^0\to\mu^+\mu^-)}{|s-M_Z^2 + i\Gamma_{tot}M_Z|^2} \qquad (I.54)$$

Note that the proportionality factor is 12π not 4π since the Z^0 has spin 1. Integrating over the resonance gives a measure of the leptonic width. One has

$$I = \int d\sqrt{s}\ \sigma(e^+e^- \to \mu^+\mu^-) = 12\pi\Gamma^{-2}(Z^0 \to l^+l^-) \int d\sqrt{s} \frac{1}{|s-M_Z^2 + i\Gamma_{tot}M_Z|^2} \qquad (I.55)$$

$$= \frac{6\pi^2\Gamma^{-2}(Z^0\to l^+l^-)}{M_Z^2\,\Gamma_{tot}}$$

Experimentally, the main source of error on the measurement of I will come from not knowing the absolute normalization of the cross section, coming from uncertainties in the

luminosity. The intrinsic errors in the total width are less important. Blondel at al[13] estimate that the overall uncertainty in $\delta I/I$ will be at the 3% level, leading to an uncertainty in the leptonic width at the 2% level:

$$\frac{\delta\Gamma(Z^0\to l^+l^-)}{\Gamma(Z^0\to l^+l^-)} \simeq 2\% \qquad \text{(I.56)}$$

This error is too large to allow one to obtain an accurate determination of $\sin^2\theta_W$, from this measurement. Using Eq(I.20b) one has

$$\delta\sin^2\theta_W \simeq \frac{1}{8}\left(\frac{\delta\Gamma(Z^0\to l^+l^-)}{\Gamma(Z^0\to l^+l^-)}\right)\frac{1}{(1-4\sin^2\theta_W)} \qquad \text{(I.57)}$$

For $\sin^2\theta_W = 0.23$, the above formula implies, for the error given in (I.56), $\delta\sin^2\theta_W \simeq 0.03$. Clearly, this is extremely poor. There are much better ways to determine $\sin^2\theta_W$ at LEP 100! Before proceeding with a discussion of how one goes about determining $\sin^2\theta_W$ accurately, it behooves us, however, to understand clearly the role which electroweak radiative corrections play in these measurements. I turn to this topic next.

Ib THE Z^0 MASS AND RADIATIVE CORRECTIONS

In the standard Glashow Salam Weinberg model[1], in lowest order, one encounters the Weinberg angle in at least four different ways:

i) It relates the SU(2) and U(1) coupling constants to e:

$$e = g\sin\theta_W = g'\cos\theta_W \qquad \text{(I.58)}$$

ii) For doublet Higgs breaking, it relates the W and Z masses (c.f. Eq I.19)

$$\sin^2\theta_W = 1 - \frac{M^2_W}{M^2_Z} \qquad \text{(I.59)}$$

iii) It appears in the relation between the Fermi constant and the W mass (c.f. Eq I.18)

$$\frac{G_F}{\sqrt{2}} = \frac{e^2}{8\sin^2\theta_W M^2_W} \qquad \text{(I.60)}$$

iv) It enters in the definition of the neutral current (c.f. Eq I.10)

$$J^\mu_{NC} = 2(J^\mu_3 - \sin^2\theta_W J^\mu_{em}) \qquad \text{(I.61)}$$

Because of this last definition, for instance, the cross section ratio among the purely NC processes $\nu_\mu e \to \nu_\mu e$ and $\bar\nu_\mu e \to \bar\nu_\mu e$ can be expressed entirely in terms of the Weinberg angle:

$$\frac{\sigma(\nu_\mu e \to \nu_\mu e)}{\sigma(\bar{\nu}_\mu e \to \bar{\nu}_\mu e)} = \frac{3 - 12\sin^2\theta_W + 16\sin^4\theta_W}{1 - 4\sin^2\theta_W + 16\sin^4\theta_W} \qquad (I.62)$$

To lowest order in the electroweak theory all these ways of expressing $\sin^2\theta_W$ are equivalent. However, this is no longer true when $O(\alpha)$ corrections are included. It is clearly more useful to focus on expressions that relate $\sin^2\theta_W$ to measurable quantities, like M_W^2/M_Z^2 or the cross section ratio (I.62), than on the definition (I.58), which relates the Weinberg angle to coupling constants which must, in turn, be defined themselves. In fact, if we used the definition (I.58) for θ_W we would find infinite contributions in higher order, which can only be eliminated through an appropriate redefinition of the coupling constants. Clearly no such problems exist if $\sin^2\theta_W$ is defined in terms of measurable quantities.

Let me try to be a bit more precise. Consider calculating the cross section for $\nu_\mu e$ scattering beyond lowest order, by summing the set of graphs shown in Fig I.11. In doing

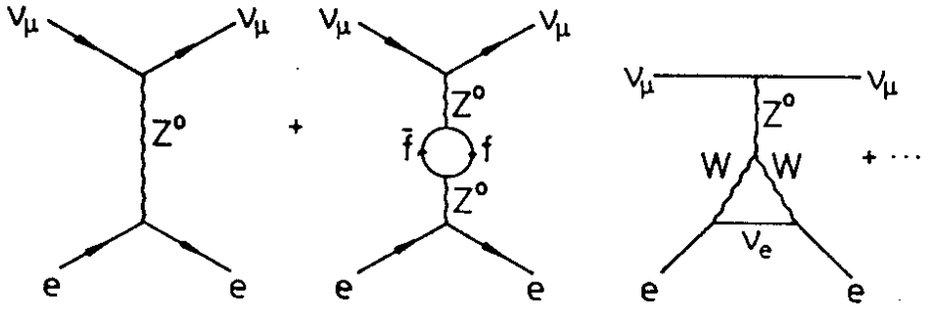

Fig I.11: Some of the graphs entering in the calculation of $\nu_\mu e$ scattering

so, one encounters, unavoidably, some infinite expressions. However, because the standard model is renormalizable, these infinities can be absorbed in a redefinition of couplings and of the breakdown scale of SU(2)xU(1). One can, in fact, choose these redefinitions in such a way that the renormalized $\sin^2\theta_W$ (which I shall denote as $\sin^2\theta_W^R$) is defined through the requirement that the cross section ratio $\sigma(\nu_\mu e \to \nu_\mu e) / \sigma(\bar{\nu}_\mu e \to \bar{\nu}_\mu e)$ to $O(\alpha)$ is given by a formula identical to (I.62):

$$\left.\frac{\sigma(\nu_\mu e \to \nu_\mu e)}{\sigma(\bar{\nu}_\mu e \to \bar{\nu}_\mu e)}\right|_{\text{to } O(\alpha)} = \frac{3 - 12\sin^2\theta_W^R + 16\sin^2\theta_W^R}{3 - 4\sin^2\theta_W^R + 16\sin^2\theta_W^R} \qquad (I.63)$$

Having done this, however, when one computes mass shifts for the W and Z bosons, by summing the vacuum polarization graphs of Fig I.12, the way to readsorb infinities is now fixed! So the ratio between the W and Z masses is now expressed in terms of $\sin^2\theta_W^R$ and calculable $O(\alpha)$ corrections.

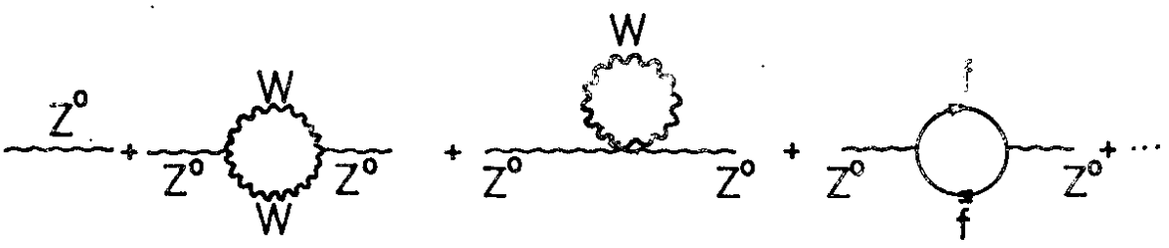

Fig I.12 vacuum polarization graphs contributing to the Z boson mass shift

That is, to O(α), Eq(I.59) gets replaced by

$$1 - \frac{M_W^2}{M_Z^2} = \sin^2\theta_W^R \, [\, 1 + c\alpha \,] \tag{I.64}$$

where c is a calculable finite constant. Of course, one could have done things in another way and absorbed the infinities associated with the graphs of Fig I.12 by adopting as a definition of the renormalized Weinberg angle (which I shall call $\sin^2\theta_W^{Mass}$) to O(α) that given by the W-Z mass ratio:

$$\sin^2\theta_W^{Mass}\Big|_{\text{to O}(\alpha)} = 1 - \frac{M_W^2}{M_Z^2} \tag{I.65}$$

This definition is different than the one adopted in (I.63) but the relationship between these two renormalized Weinberg angles is well defined and calculable. In fact, from (I.64), one has

$$\sin^2\theta_W^{Mass} = \sin^2\theta_W^R \, [1 + c\alpha] \tag{I.66}$$

For the purposes of computing radiative corrections in the SLC/LEP energy range, it is most useful to use as a definition of the renormalized Weinberg angle that given by the W-Z mass ratio (I.65), a suggestion which was originally advocated by Sirlin[20]. For ease in writing I shall, henceforth, drop the superscript "Mass" from $\sin^2\theta_W^{Mass}$, but it is to be understood, from now on that

$$\sin^2\theta_W \equiv 1 - \frac{M_W^2}{M_Z^2} \tag{I.67}$$

One can obtain a value for $\sin^2\theta_W$ from the direct measurements of M_W and M_Z at the CERN collider. Because what enters in (I.67) is the ratio of these masses, the large systematic errors associated with the energy calibration cancel. However, the statistical errors are still large enough so that the value obtained for $\sin^2\theta_W$ is not too precise. Using for M_W and M_Z the values given in the recent review of di Lella[21]:

$$M_W = (83.5 \, {}^{+\,1.1}_{-\,1.0} \pm 2.8)\text{GeV} \qquad UA_1 \tag{I.68a}$$

$$M_W = (81.2 \pm 1.1 \pm 1.3)\text{GeV} \qquad UA_2 \tag{I.68b}$$

$M_Z = (93.0 \pm 1.4 \pm 3.2)\text{GeV}$ UA_1 (I.68c)

$M_Z = (92.5 \pm 1.3 \pm 1.5)\text{GeV}$ UA_2 (I.68d)

one obtains, taking only the statistical errors into account,

$\sin^2\theta_W = 0.194 \pm 0.031$ UA_1 (I.69a)

$\sin^2\theta_W = 0.229 \pm 0.030$ UA_2 (I.69b)

which gives as average for the collider

$$\sin^2\theta_W = 0.212 \pm 0.022 \quad \text{(I.70)}$$

A much more precise value for $\sin^2\theta_W$ can be extracted from low energy neutral current experiments, after including $O(\alpha)$ electroweak radiative corrections. These corrections were computed in 1981 by Marciano and Sirlin[22] and Llewellyn Smith and Wheater[23]. These authors, using the world average uncorrected value for $\sin^2\theta_W$ from the compilation of Kim et al[24]

$$(\sin^2\theta_W)_{\text{uncorrected}} = 0.229 \pm 0.011 \quad \text{(I.71)}$$

arrived at a value of the Weinberg angle[22,23]:

$$(\sin^2\theta_W) = 0.217 \pm 0.014 \quad \text{(I.72)}$$

The slight difference in the errors in (I.71) and (I.72) reflects the fact that some theoretical uncertainties are also folded in (I.72).

Five years later, the situation with respect to the value of $\sin^2\theta_W$, extracted from deep inelastic experiments, has considerably improved. First of all, much more neutral current data has been collected. Secondly, the individual experiments themselves have done the radiative corrections on their own data, avoiding thereby the pitfalls inherent in doing radiative corrections to averaged data. The result is a trend toward a higher central value for $\sin^2\theta_W$, than the value obtained by Marciano and Sirlin[22] and Llewellyn Smith and Wheater[23], and a reduced error. There is still a fair theoretical uncertainty from various parton model assumptions necessary for the analysis: sea content, value of m_c, etc., which probably add to an irreducible theoretical error in $\sin^2\theta_W$ of $\pm$ 0.005. I quote below a compilation by Panman[25] of the most recent values for $\sin^2\theta_W$ from deep inelastic neutrino scattering experiments at Fermilab and CERN:

$\sin^2\theta_W = 0.239 \pm 0.008 \pm 0.006$ CCFRR (I.73a)

$$\sin^2\theta_W = 0.246 \pm 0.011 \pm 0.012 \qquad \text{FNMF} \qquad \text{(I.73b)}$$

$$\sin^2\theta_W = 0.225 \pm 0.005 \qquad \text{CDHS} \qquad \text{(I.73c)}$$

$$\sin^2\theta_W = 0.236 \pm 0.005 \qquad \text{CHARM} \qquad \text{(I.73d)}$$

The Fermilab experiments give both statistical and systematic errors, while the error for the CERN experiments is a combined error. These results lead to an average value for $\sin^2\theta_W$ in 1986 of[25]

$$\sin^2\theta_W = 0.233 \pm 0.004 \pm 0.005 \qquad \text{(I.74)}$$

where the last error above is an estimate of the theoretical uncertainty. The biggest source of this uncertainty is the value of the charmed quark mass, used in the analysis. The results given use $m_c = 1.5$ GeV but, for example, CDHS[26] quotes a dependence of $\sin^2\theta_W$ on m_c

$$\delta\sin^2\theta_W = 0.013\ (m_c(\text{GeV}) - 1.5) \qquad \text{(I.75)}$$

It is clear that the directly computed value for $\sin^2\theta_W$ obtained at the collider, Eq(I.70), is in perfect agreement with the value obtained in $\nu_\mu N$ scattering, after radiative corrections have been applied, Eq(I.74). This agreement, however, is not really yet a test of the electroweak radiative corrections. The errors in Eq(I.70) are far too big, so that this value also agrees with the uncorrected value of $\sin^2\theta_W$! LEP and the SLC will allow for a much more stringent test of the electroweak radiative corrections by providing a precise value for M_Z and $\sin^2\theta_W$ (LEP 100, SLC) and M_W (LEP 200). Accurate knowledge of two of these quantities, either M_Z and $\sin^2\theta_W$, or M_W and $\sin^2\theta_W$, or M_Z and M_W, tests directly these higher order corrections. As this is an important part of the physics potential of LEP, let me try to clarify this point with some care.

Eq(I.60) gives the lowest order interrelation between the Fermi constant and the W mass. Adopting the definition (I.67) for $\sin^2\theta_W$, radiative corrections modify this formula to [27]

$$M^2_W = \frac{\pi\alpha}{\sqrt{2}\, G_\mu \sin^2\theta_W} \; \frac{1}{(1 - \Delta r)} \qquad \text{(I.76)}$$

Here Δr is a theoretically computable shift[27], to be discussed in more detail below, which is of the order of 7%; α is the fine structure constant ($\alpha \simeq 1/137$) and G_μ is the Fermi constant measured in μ decay, in which certain purely electromagnetic corrections are incorporated[28]. Specifically

$$\frac{1}{\tau_\mu} = G^2_\mu \left[\left(1 - \frac{8m_e^2}{m_\mu^2}\right)\left(1 + \frac{3m_\mu^2}{5M_W^2}\right) \frac{m_\mu^5}{192\pi^3}\right] \text{pem} \qquad \text{(I.77)}$$

with

$$\rho^{em} = 1 + \frac{\alpha}{2\pi}\left(\frac{25}{4} - \pi^2\right)\left[1 + \frac{2\alpha}{3\pi}\ln\frac{m_\mu}{m_e}\right] \qquad (I.78)$$

Since α and G_μ are known to great accuracy[29]

$$\alpha^{-1} = 137.03604 \pm 0.00011$$
$$G_\mu = (1.16637 \pm 0.00002) \times 10^{-5}\ \text{GeV}^{-2} \qquad (I.79)$$

the test of the radiative corrections - the Δr term in Eq(I.76) - will depend on a precision measurement of <u>both</u> M_W and $\sin^2\theta_W$. However, since $\sin^2\theta_W$, M_W and M_Z are related by (I.67) any pair of these quantities will do. Using the average value for $\sin^2\theta_W$ from neutrino scattering experiments (Eq I.74) and the UA_1 - UA_2 average value for M_W

$$\langle M_W \rangle = 82.35 \pm 1.7\ \text{GeV} \qquad (I.80)$$

gives for (Δr) today a value which is consistent with the theoretical predictions, but which is only $2^{1/2}\ \sigma$ away from zero:

$$(\Delta r)_{exp} = 0.12 \pm 0.05 \qquad (I.81)$$

LEP and the SLC can reduce the uncertainty in the value of Δr to $\delta\Delta r = \pm 0.01$. Knowledge of Δr to this accuracy can begin to probe very interesting aspects of the standard model, as will be seen below.

The magnitude of the correction Δr has an origin which can be readily understood physically[30]. In Eq(I.76), two of the parameters, α and G_μ, are specified from experiments done at low q^2. On the other hand, both M_W and $\sin^2\theta_W$ are quantities that involve a scale of order 100 GeV. Radiative corrections can only be large if there are large logarithms: $\alpha/\pi \ln M_W^2/\langle q^2\rangle$, since α itself is a small parameter. So if we replaced α and G_μ by their running values $\alpha(M_W^2)$ and $G_\mu(M_W^2)$ in Eq(I.76), since all quantities are now evaluated at the same scale, the bulk of the large radiative effects should be accounted for. Thus

$$M_W^2 = \frac{\pi\alpha}{\sqrt{2}G_\mu \sin^2\theta_W(1-\Delta r)} \approx \frac{\pi\alpha(M^2_W)}{\sqrt{2}G_\mu(M_W^2)\sin^2\theta_W} \qquad (I.82)$$

Actually the Fermi constant, defined through μ-decay, does not run. The effective Lagrangian for this process, after performing a Fierz transformation analogous to that done in (I.50), reads

$$\mathcal{L}^{eff} = \frac{G_F}{\sqrt{2}}\bar{\mu}\gamma_\mu(1-\gamma_5)e\,\bar{\nu}_e\gamma^\mu(1-\gamma_5)\nu_\mu \qquad (I.83)$$

The second current in (I.83) is inert to electromagnetic radiative corrections, while the first current has no anomalous dimensions, since it is conserved in the massless limit. So G_F does not get corrected by $\alpha \ln M^2_W/m^2_\mu$ terms in higher order. (This is also clear from Eq I.78) and one has

$$G_\mu (M^2_W) \simeq G_\mu \tag{I.84}$$

Hence one is lead to expect[30]

$$M^2_W \simeq \frac{\pi\alpha(M^2_W)}{\sqrt{2}G_\mu \sin^2\theta_W} \tag{I.85}$$

Computing $\alpha(M^2_W)$ through the usual QED vacuum polarization contributions gives[30]

$$\alpha(M^2_W) \simeq \frac{1}{128} \simeq \alpha\left(\frac{137}{128}\right) = \alpha[1+0.07)] \tag{I.86}$$

which in view of (I.82) leads to $\Delta r \simeq 0.07$. The result of a detailed calculation[27] is in (almost too good) agreement with this qualitative discussion, giving

$$\Delta r = 0.0696 \pm 0.00020 \tag{I.87}$$

for $m_t = 36$ GeV and using a value for the Higgs mass $M_H = M_Z$. The small error in (I.87) is due to errors in the cross section $e^+e^- \to$ hadrons, used to estimate the vacuum polarization contributions of light quarks.

The level of accuracy for Δr, $\delta\Delta r = \pm 0.01$, which I will show is achievable at LEP, is the level needed to begin probing some of the yet unknown parameters of the standard model. If the t quark is heavier than 45 GeV or so, it will not be seen directly in Z^0 decays, but it can affect Δr. One finds[27], approximately,

$$\delta(\Delta r)^{top} \simeq -0.007 \left[\frac{m_t^2 - (40\ \text{GeV})^2}{M^2_W}\right] \tag{I.88}$$

So a 100 GeV top quark will decrease Δr by 0.01, and a 250 GeV top will totally erase Δr. Present data, Eq(I.81), already disfavors such a possibility. The dependence of Δr on M_H is milder, being only logarithmic. Nevertheless, since, approximately[27],

$$\delta(\Delta r)^{Higgs} \simeq 0.0024 \ln M^2_H/M^2_Z \tag{I.89}$$

one sees that, if $M_H = 1$ TeV, Δr increases by 0.01. So clearly an accuracy of Δr to ± 0.01 is very desirable. At LEP 100 such a precision measurement is possible through an accurate determination of M_Z and a very precise study of the forward-backward asymmetry in the process $e^+e^- \to \mu^+\mu^-$, which will determine $\sin^2\theta_W$. At LEP 200, these measurements can be com-

plemented by an equally accurate determination of M_W. We discuss the first two points below and defer a discussion of the M_W measurements to section II.

The accuracy with which M_Z can be determined at LEP has been discussed by Blondel et al[13] in the Yellow report. Even though M_Z cannot just be determined by the location of the peak in $e^+e^- \to \mu^+\mu^-$, since this is shifted by radiative effects, the statistical errors that follow from a fit of the radiative corrected line shape are negligible: $(\delta M_Z)_{Stat} \lesssim$ 10 MeV. The systematic error on M_Z is dominated by the determination of the absolute energy scale and by a possible linear variation of the luminosity over the Z^0 peak region. A linear variation in $\mathcal{L}$ of 2% over 10 GeV - which is a reasonable estimate - would give a systematic shift in M_Z of ~ 10 MeV. Of more concern is the absolute calibration of the LEP energy. The error arising from magnet calibrations will limit the accuracy with which the beam energy will be known to[13] $\delta E/E \simeq 3\times10^{-4}$, implying $(\delta M_Z)_{syst} \simeq 30$ MeV. Transversly polarized beams at LEP, in principle, can allow an accurate determination of the spin precession frequency of the electrons which, in turn, can be used to infer the beam energy more precisely. (An accuracy of the order of 10^{-4} is quoted in Ref 13). At any rate, it is probably fair to conclude that experimental errors on M_Z at LEP should give at most an uncertainty:

$$(\delta M_Z)_{exp} \lesssim 50 \text{ MeV} \tag{I.90}$$

Since

$$\delta\Delta r = 2(1-\Delta r)\frac{\delta M_Z}{M_Z} \tag{I.91}$$

the error on Δr from $(\delta M_Z)_{exp}$ is very small ($\delta\Delta r \simeq 0.001$). So the main uncertainty in Δr at LEP 100 will arise from errors in $\sin^2\theta_W$. One has, using

$$(1-\Delta r) = \frac{\pi\alpha}{\sqrt{2}G_\mu \sin^2\theta_W \cos^2\theta_W M_Z^2} \tag{I.92}$$

that

$$\delta\Delta r = \frac{(\cos^2\theta_W - \sin^2\theta_W)(1-\Delta r)}{\cos^2\theta_W \sin^2\theta_W}\,\delta(\sin^2\theta_W) \simeq \frac{8}{3}\,\delta(\sin^2\theta_W) \tag{I.93}$$

So to achieve an error in Δr of 0.01 one needs to measure $\sin^2\theta_W$ at LEP 100 with an accuracy of $\pm$ 0.004. This is the accuracy with which we know experimentally $\sin^2\theta_W$ in deep inelastic neutrino scattering. Unfortunately, in this latter measurements, there is also an irreducible theoretical error of $\pm$ 0.005. Such an error will not be present at LEP and SLC since $\sin^2\theta_W$ will be extracted from a purely leptonic process: $e^+e^- \to \mu^+\mu^-$.

Ic FORWARD-BACKWARD ASYMMETRY AND GSW PRECISION TESTS

Studying the asymmetry between events produced in the forward and backward regions for the process $e^+e^- \to \mu^+\mu^-$ one can extract a value for $\sin^2\theta_W$. If we define the angle θ as the

angle between the produced μ^- and the direction of the incident e^- (see Fig I.13), then forward corresponds to $0 \leq \theta \leq \pi/2$.

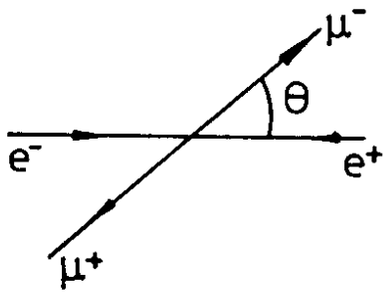

Fig I.13 Kinematics for $e^+e^- \to \mu^+\mu^-$

One can compute this forward-backward asymmetry, A_{FB}, rather simply in lowest order, via the graphs of Fig I.4. Radiative corrections to this result have been calculated by Lynn and Stuart[31] and Wetzel[32]. As Consoli and Sirlin[33] point out, one can absorb quite a lot of the $O(\alpha)$ weak corrections by expressing $(A_{FB})_{\text{lowest order}}$ using the physical value of $\sin^2\theta_W = 1 - M^2_W/M^2_Z$. Thus one can imagine splitting the results of the calculation into three pieces

$$A_{FB} = (A_{FB})_{\text{lowest order}} + \delta A_{FB}^{\text{weak}} + \delta A_{FB}^{\text{QED}} \qquad (I.94)$$

I will explicitly display an expression for the first term in the RHS of Eq(I.94). The weak correction to A_{FB} can be extracted from the results of Ref 31 and 32. Finally, one should remember that there is also a purely electromagnetic correction to A_{FB}, since this quantity is not a parity violating asymmetry. This last term depends, however, on experimental cuts. Since $(A_{FB})_{\text{lowest order}}$ is an explicit function of $\sin^2\theta_W$, once $\delta A_{FB}^{\text{weak}}$ and $\delta A_{FB}^{\text{QED}}$ are subtracted away from the measured forward-backward asymmetry, the result will yield directly a value for the Weinberg angle.

A straightforward calculation of the lowest order contribution to the angular distribution for $e^+e^- \to \mu^+\mu^-$ gives:

$$\frac{d\sigma}{d\cos\theta} = \frac{2\pi\alpha^2}{s} \left\{ (1 + \cos^2\theta)\, F_1(s) + 2\cos\theta\, F_2(s) \right\} \qquad (I.95)$$

where

$$F_1(s) = 1 + \frac{2s(s-M_Z^2)}{(s-M_Z^2)^2 + M_Z^2\,\Gamma_{tot}^2} \cdot \frac{V_e^2}{\sin^2\theta_W \cos^2\theta_W} + \frac{s^2}{(s-M_Z^2)^2 + M_Z^2\,\Gamma_{tot}^2} \cdot \frac{(V_e^2 + A_e^2)^2}{\sin^4\theta_W \cos^4\theta_W} \qquad (I.96)$$

and

$$F_2(s) = \frac{2s(s-M_Z^2)}{(s-M_Z^2)^2 + M_Z^2\,\Gamma_{tot}^2}\;\frac{A_e^2}{\sin^2\theta_W\cos^2\theta_W} + \frac{4s^2}{(s-M_Z^2)^2 + M_Z^2\,\Gamma_{tot}^2}\;\frac{V_e^2\,A_e^2}{\sin^4\theta_W\cos^4\theta_W} \qquad (I.97)$$

The forward-backward asymmetry is then, simply,

$$A_{FB} = \frac{\int_0^1 d\cos\theta\left(\frac{d\sigma}{d\cos\theta}\right) - \int_{-1}^0 d\cos\theta\left(\frac{d\sigma}{d\cos\theta}\right)}{\int_0^1 d\cos\theta\left(\frac{d\sigma}{d\cos\sigma}\right) + \int_{-1}^0 d\cos\theta\left(\frac{d\sigma}{d\cos\theta}\right)} = \frac{3F_2(s)}{4F_1(s)} \qquad (I.98)$$

At $\sqrt{s} = M_Z$, dropping terms of $O((\Gamma_Z/M_Z)^2)$, one has

$$A_{FB}\Big|^{\text{lowest order}}_{\sqrt{s}=M_Z} \simeq \frac{3V_e^2\,A_e^2}{(V_e^2 + A_e^2)^2} \simeq 3(1-4\sin^2\theta_W)^2 \qquad (I.99)$$

Because $\sin^2\theta_W$ is near 1/4, unfortunately this asymmetry is quite small. Furthermore since (1.99) depends quadratically on V_e^2, the accuracy required on A_{FB} to determine $\sin^2\theta_W$ precisely depends on the actual value of $\sin^2\theta_W$

$$\delta A_{FB}\Big|^{\text{lowest order}}_{\sqrt{s}=M_Z} = 24[1 - 4\sin^2\theta_W]\,\delta\sin^2\theta_W \qquad (I.100)$$

For $\sin^2\theta_W = 0.233$, for example, one needs an accuracy $\delta A_{FB} = 0.0065$ to determine $\sin^2\theta_W$ to $\pm$ 0.004, corresponding then to $\delta\Delta r = 0.01$. This is quite a hard task if one remembers that at PETRA, at $\sqrt{s} \simeq 34$ GeV where there is the most data, the typical error on a 10% forward-backward asymmetry was about $\pm$ 2%. Here one will be dealing with a 2% asymmetry and one wants 3 times the accuracy. Nevertheless, a study of this question at LEP[34] indicates that with 40 days of running at a luminosity of 10^{31} cm^{-2} sec^{-1} one could achieve a statistical error on $\delta A_{FB} \simeq 0.005$, which could be reduced to 0.002 with 200 days of running. However, the effect of systematic uncertainties is much harder to judge.

In addition to purely experimental uncertainties, there are also some theoretical problems to worry about:

1) As long as $\sin^2\theta_W$ is not too near 1/4, δA_{FB}^{weak} is not too large a correction to $\left(A_{FB} \right)_{lowest\ order}$ [33]. However, this is still a correction that must be included to extract an accurate value for $\sin^2\theta_W$. In practice, as advocated by Lynn, Peskin and Stuart[35], one should really avoid separating A_{FB} this way. A more sensible way to check radiative effects in SU(2)xU(1) may be to look at the predictions for $A_{FB} - \delta A_{FB}^{QED}$ as a function of the Z^0 mass, for various choices of parameters (m_t, M_H) which enter in Δr. In a plot of $A_{FB} - \delta A_{FB}^{QED}$ vs M_Z, the predictions of the standard model will span a band (see Fig I.14, for an illustration). The question then is whether the experimentally obtained result sits in the allowed band or not?

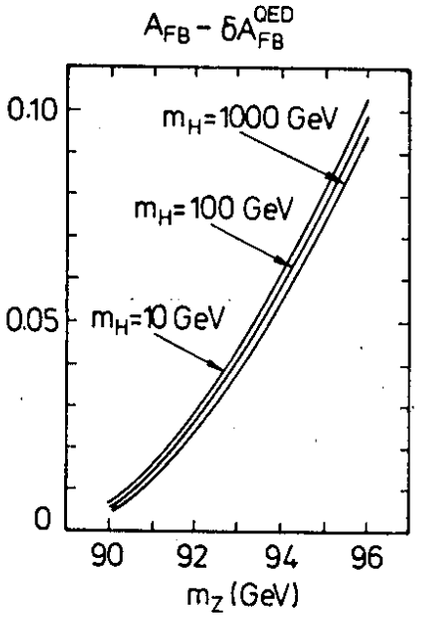

Fig I.14: $A_{FB} - \delta A_{FB}^{QED}$ as a function of M_Z for various values of M_H and m_t = 30 GeV. From Ref. 31

2) The purely QED part of the forward-backward asymmetry must be extracted carefully to really check the purely electroweak radiative effects. This is somewhat tricky for two reasons[4)12)]:

i) The actual value for δA_{FB}^{QED} depends in detail on the cuts[12] made for the process $e^+e^- \to \mu^+\mu^-(\gamma)$, and so is apparatus dependent

ii) Typically, $\delta A_{FB}^{QED} \sim 0.02 - 0.03$[12] at $\sqrt{s} = M_Z$ which is of the size of the effect, but is 3 - 5 times the size of the desired accuracy on A_{FB}. So it is likely that one will have to include higher order in α QED corrections to achieve the desired accuracy[26].

My impression is that life will be very difficult and that to extract a precise value for Δr will require many years of careful measurements. In addition, unambiguous results will not really be obtained unless one is able to establish a symbiotic theorist-experimentalist relationship.

The forward-backward asymmetry in $e^+e^- \to \mu^+\mu^-$ is not the only way in which one can measure a value for $\sin^2\theta_W$ at the Z^0 peak. Asymmetries involving helicity measurements, if

feasible, turn out to be particularly sensitive to the Weinberg angle. For instance, the polarization asymmetry, A_{pol}, which measures the difference in cross section for producing left, or right, polarized fermions is proportional to the vector coupling of the outgoing fermion. This asymmetry can be measured in the case of the process $e^+e^- \to \tau^+\tau^-$, since one can use the decay $\tau^- \to \pi^-\nu_\tau$ as a polarization analyzer. The lowest order asymmetry is easily calculated to be

$$A_{pol}\Big|^{\text{lowest order}}_{\sqrt{s}=M_Z} = \frac{\sigma(\tau_L^-) - \sigma(\tau_R^-)}{\sigma(\tau_L^-) + \sigma(\tau_R^-)}\Bigg|_{\sqrt{s}=M_Z}$$

$$\simeq \frac{2\, V_\tau\, A_\tau}{(V_\tau^2 + A_\tau^2)} = 2(1 - 4\sin^2\theta_W) \qquad \text{(I.101)}$$

Eq(I.101), in contrast to Eq(I.99), is linear in $1 - 4\sin^2\theta_W$. Thus the error in $\sin^2\theta_W$ is independent of the precise value of the Weinberg angle:

$$\delta\sin^2\theta_W = \frac{1}{8}\,\delta A_{pol} \qquad \text{(I.102)}$$

Furthermore, to obtain an error $\delta\sin^2\theta_W = \pm 0.004$, a much less precise value of A_{pol} is needed ($\delta A_{pol} \simeq 0.03$) and the polarization asymmetry itself is much bigger than A_{FB} ($A_{pol} \simeq 0.15$ vs $A_{FB} \simeq 0.02$). Unfortunately, the measurement itself of Apol is considerably more difficult.

The way in which A_{pol} for τ^- leptons can be measured is by looking at the energy distribution of the produced pions, in the decay $\tau^- \to \pi^-\nu_\tau$. In the rest frame of the τ leptons, the decay $\tau^- \to \pi^-\nu$ is forbidden for ν_τ's produced along the direction of the τ^- polarization, as shown in Fig I.15.

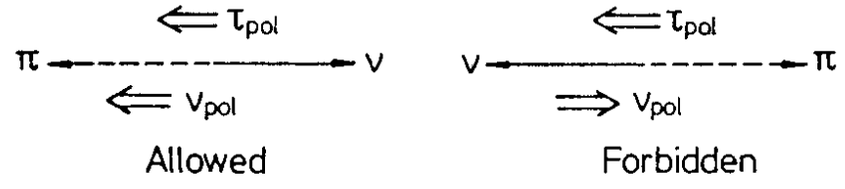

Fig I.15. Allowed and forbidden configurations in $\tau^- \to \pi^-\nu_\tau$ decays.

If θ_π is the angle which the pion makes in the τ rest frame with respect to the τ direction in the laboratory, then it is easy to see that the angular distribution of the produced pions in the τ rest frame is given by

$$\frac{dN}{d\cos\theta_\pi} \sim (1 - A_{pol}\cos\theta_\pi) \qquad \text{(I.103)}$$

Since the pion energy in the laboratory is related to θ_π by

$$x_\pi = \frac{E_\pi}{E_{beam}} \simeq \frac{1}{2}(1 + \cos\theta_\pi) \qquad (I.104)$$

it follows that a measurement of the distribution dN/dx_π will give a direct estimate of A_{pol}:

$$\frac{dN}{dx_\pi} \sim [1 - A_{pol}(2x_\pi - 1)] \qquad (I.105)$$

Chaveau[37], in the Yellow report, estimates that with a run of 100 days one can achieve a statistical accuracy on the τ polarization asymmetry of $(\delta A_{pol})^{stat} \sim 0.016$ with a systematic error of half this amount. If this can be achieved, this measurement could provide an extremely accurate value for $\sin^2\theta_W$. But even if the accuracy were reduced by half, one would still achieve the goal of measuring $\delta\sin^2\theta_W$ to $\pm$ 0.004.

If one were able to have longitudinally polarized beams (something which might be easier to achieve at SLC than at LEP) then a measurement of the left-right asymmetry for the process $e^+e^- \to \mu^+\mu^-$ would also give a sensitive measurement of $\sin^2\theta_W$. At resonance and using only the lowest order contributions, one finds[4)35)]

$$A_{LR} = \frac{\sigma(e_L^-) - \sigma(e_R^-)}{\sigma(e_L^-) + \sigma(e_R^-)} \simeq 2P_e(1 - 4\sin^2\theta_W) \qquad (I.106)$$

where P_e is the electron polarization. So the comments made for A_{pol} apply essentially verbatim here, provided P_e is large. The presence of a non vanishing longitudinal polarization, furthermore, modifies the formula (Eq I.99) for the forward-backward asymmetry, so that this asymmetry does not vanish anymore quadratically for $\sin^2\theta_W = 1/4$. One finds[4)], in lowest order and at $\sqrt{s} = M_Z$,

$$A_{FB} \simeq \frac{3}{2}(1 - 4\sin^2\theta_W)[P_e + 2(1 - 4\sin^2\theta_W)] \qquad (I.107)$$

So the ability of doing measurements with longitudinally polarized beams may help achieve a more reliable value for $\sin^2\theta_W$.

As a last topic of this already rather long section, I want to briefly discuss radiative corrections to the Z^0 partial widths. These widths also receive $O(\alpha)$ modifications and, for the leptonic channels, one can write:

$$\Gamma(Z^0 \to \nu\bar{\nu}) = \frac{G_\mu M_Z^3}{12\sqrt{2}\pi}(1 + \varepsilon_{\nu\bar{\nu}})$$

$$\Gamma(Z^0 \to e^+e^-) = \frac{G_\mu M_Z^3}{6\sqrt{2}\pi}(1 + (1 - 4\sin^2\theta_W)^2)(1 + \varepsilon_{ee}) \qquad (I.108)$$

The corrections $\varepsilon_{\nu\bar{\nu}}$ and ε_{ee} have been computed by Consoli, Lo Presti and Maiani[11] and by Wetzel[38] and they are quite small. This is understandable, since G_μ does not run so that one expects $\varepsilon_{\nu\bar{\nu}}$, $\varepsilon_{ee} \sim \frac{\alpha}{\pi}$. Indeed, typically one finds[11)38)] $\varepsilon_{\nu\bar{\nu}}$, $\varepsilon_{ee} \sim (2\text{-}3)\times 10^{-3}$. These corrections are very much below the experimental error one can hope to achieve on the partial widths (recall Eq I.S6). Therefore, for all practical purposes, these corrections can be ignored completely.

II. ELECTROWEAK PHYSICS WITH W PAIRS

At LEP 200 the process $e^+e^- \to W^+W^-$ will become kinematically accessible. In this section, I want to discuss some of the nice electroweak physics, connected with this reaction, which can be studied in this higher energy regime.

IIa GENERAL PROPERTIES OF THE REACTION $e^+e^- \to W^+W^-$

The process $e^+e^- \to W^+W^-$ is particularly interesting for two reasons:

i) It involves all three interactions of the standard model (Eq I.6), as shown in Fig II.1

ii) It is the first reaction where there will be a direct test of the three gauge vertices γW^+W^- and $Z^0W^+W^-$

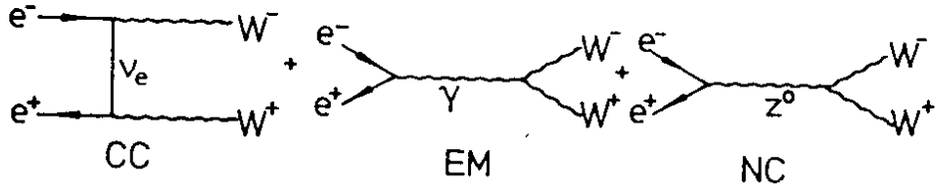

Fig II.1 Lowest order contributions to the process $e^+e^- \to W^+W^-$

The three gauge vertices are a fundamental ingredient of non Abelian gauge theories. They arise because the field strengths for non abelian gauge fields contain a term quadratic in these fields. For instance, for the SU(2) gauge fields W^μ_a, a = 1,2,3, one has

$$F^{\mu\nu}_a = \partial^\mu W^\nu_a - \partial^\nu W^\mu_a + ig\varepsilon_{abc}\, W^\mu_b\, W^\nu_c \qquad (II.1)$$

Because of this, the usual "kinetic energy" form of the gauge field Lagrangian

$$\mathcal{L} = -\frac{1}{4} F^{\mu\nu}_a F_{a\mu\nu} \qquad (II.2)$$

implies both trilinear and quadrilinear gauge couplings. The effect of these couplings is felt indirectly through their contribution to virtual higher order corrections. However, LEP 200 is the first place where there will be the possibility of verifying directly the presence of these trilinear gauge couplings, in a lowest order process.

The gauge boson W_3^μ is a linear combination of the photon and Z^0 fields. One has

$$W_3^\mu = \cos\theta_W Z^\mu + \sin\theta_W A^\mu \qquad \text{(II.3)}$$

Because the trilinear gauge couplings arise only from the SU(2) gauge interactions, it is clear that the γW^+W^- and $Z^0W^+W^-$ vertices are related to each other. Since

$$W_\pm^\mu = \frac{1}{\sqrt{2}} (W_1^\mu \mp iW_2^\mu) \qquad \text{(II.4)}$$

one easily deduces from Eqs (II.2) and (II.3) the following VW^+W^- vertex, where $V = \begin{cases} A, Z^0 \end{cases}$

$$\Gamma_V^{\mu\alpha\beta}(p,q,\bar{q}) = ig_{VWW} \left\{ (\bar{q}-q)^\mu \eta^{\alpha\beta} + (p-\bar{q})^\alpha \eta^{\mu\beta} + (q-p)^\beta \eta^{\mu\alpha} \right\} \qquad \text{(II.5)}$$

This vertex, with the relevant kinematical notation, is shown in Fig II.2. In the above the coupling g_{VWW}, for the Z^0 and the photon, is given by

$$g_{ZWW} = g\cos\theta_W = e\cot\theta_W$$

$$g_{AWW} = g\sin\theta_W = e \qquad \text{(II.5)}$$

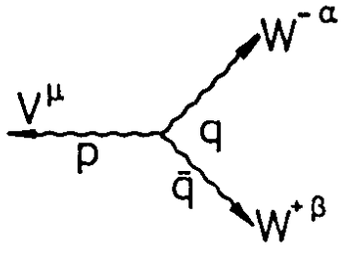

Fig II.2 The three gauge vertex VWW in momentum space. Note that $p+q+\bar{q}=0$

Using the interaction Lagrangian of Eq (I.6) along with the three gauge vertices displayed above, it is a straightforward matter to calculate the cross section for the process $e^+e^- \to W^+W^-$. This computation was first carried out, about 10 years ago, by Shuskov, Flambaum and Khriplovich[39] and by Alles, Boyer and Buras[40]. The result for the total cross section can be written as

$$\sigma = \frac{\pi\alpha^2\beta}{2s\sin^4\theta_W} \left\{ [1 + 2\lambda + 2\lambda^2] \frac{1}{\beta} \ln\left(\frac{1+\beta}{1-\beta}\right) - \frac{5}{4} \right.$$

$$+ \frac{M_Z^2(1-2\sin^2\theta_W)}{(s-M_Z^2)} \left[2(2\lambda + \lambda^2) \frac{1}{\beta} \ln\left(\frac{1+\beta}{1-\beta}\right) - \frac{1}{12\lambda} - \frac{5}{3} - \lambda \right]$$

$$\left. + \frac{M_Z^4(8\sin^4\theta_W - 4\sin^2\theta_W + 1)\beta^2}{48(s-M_Z^2)^2} \left[\frac{1}{\lambda^2} + \frac{20}{\lambda} + 12 \right] \right\} \qquad \text{(II.7)}$$

Here $\beta = (1-4\lambda)^{1/2}$, $\lambda = M_W^2/s$ and $s = (2E_b)^2$ is the square of the CM energy. This cross section is plotted versus the beam energy, E_b, in Fig II.3. As can be seen from the figure,

the cross section after the threshold rise is quite flat in the LEP 200 region. In magnitude this cross section is relatively large, of O(20 pb), which is the size of the cross section for $e^+e^- \to$ hadrons in this energy range. If one takes into account of the finite width of the W's, the rapid rise shown in Fig II.3 at threshold will be softened. We shall have occasion to return to this point below.

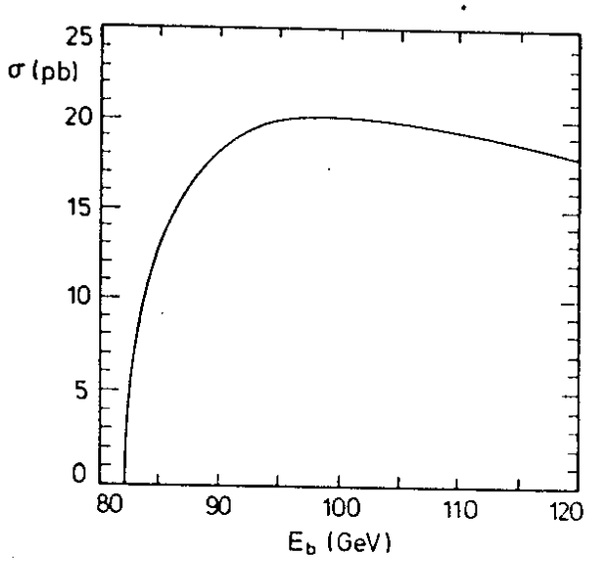

Fig II.3 Total cross section for the process $e^+e^- \to W^+W^-$ in the standard model

At LEP 200 it is reasonable to expect a somewhat higher luminosity than at LEP 100, perhaps as large as

$$\mathcal{L}_{\text{LEP 200}} = 5\times10^{31}\ \text{cm}^{-2}\text{sec}^{-1} \qquad \text{(II.8)}$$

For an "experimental" year of 10^7 sec, such a luminosity is equivalent to collecting 500 pb^{-1} of data. For the case of W production this corresponds to roughly 10^4 W^+W^- pairs per year, a very nice data sample with which to test the standard model.

The cross section given by Eq (II.7), at energies much larger than 2 M_W, falls in an essentially pointlike manner (except for a ln s factor). One easily deduces that

$$\sigma \underset{s>>M_W^2}{\sim} \frac{\pi\alpha^2}{2\sin^4\theta_W}\ \frac{1}{s}\ \ln s/M_W^2 \qquad \text{(II.9)}$$

This good asymptotic behaviour obtains only as a result of crucial cancellations provided by the presence of the graphs containing the three gauge vertices. Indeed, without the three gauge vertices in the precise form given by Eq II.5, the cross section for $e^+e^- \to W^+W^-$ would violate unitarity. For instance, the cross section arising purely from the ν-exchange graph of Fig II.1 grows linearly with s[41]

$$\sigma_{\nu \text{ exchange}} \underset{s>>M_W^2}{\sim} \frac{\pi\alpha^2 s}{96\sin^4\theta_W M_W^4} = \frac{G_F}{48\pi} s \qquad \text{(II.10)}$$

The inclusion of the other two graphs in Fig II.1, with the couplings predicted by the standard model, softens this bad behaviour to that given in Eq (II.9). Unfortunately, since LEP 200 will at most explore energies up to $E_b \simeq 100$ GeV, the difference between $\sigma_{\nu \text{ exchange}}$ and the total cross section predicted by the standard model is not overwhelming, as shown in Fig II.4.

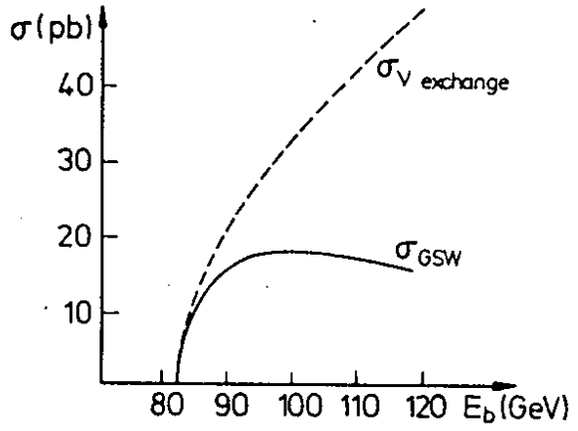

Fig II.4 Comparison of the ν-exchange cross section to that of the standard model, for the process $e^+e^- \to W^+W^-$

The unitarity of the Kobayashi Maskawa matrix V_{KM} (see Eq I.9) guarantees that the W's couple universally to quark and lepton doublets. Neglecting fermion masses and QCD corrections, it follows therefore that

$$B(W \to \text{hadrons}) \simeq \frac{3}{3+1} = \frac{3}{4} \qquad \text{(II.11)}$$

where the factor of 3 is due to color. This means that the W^+W^- signal at LEP 200 going into 4 jets is roughly half of the total W^+W^- signal

$$\sigma(e^+e^- \to W^+W^- \to 4 \text{ jets}) \simeq \frac{9}{16} \sigma(e^+e^- \to W^+W^-) \simeq 10 \text{ pb} \qquad \text{(II.12)}$$

This cross section is much bigger than the 4 jet cross section expected in QCD, which should be less, or of the order of, 0.5 pb[41]. So the W^+W^- signal manifesting itself into 4 jets at LEP 200 is almost background free! Furthermore, other channels like $e^+e^- \to W^+W^-$, with one of the W's decaying leptonically, are also quite distinctive, with very little background. It is thus reasonable to presume that with roughly 10^4 W^+W^- events produced per year one should be able to do detailed investigations with about 5000 W^+W^- pairs per year, per experiment. This will be a unique sample to study the three gauge vertex in the foreseeable future. Although this vertex enters also in the production of W pairs in pp or $\bar{p}p$ collisions, the study of these events is precluded by enormous backgrounds in hadronic machines[41]. These backgrounds are non existent at LEP 200.

Not only the total cross section but also the angular distribution for the process $e^+e^- \to W^+W^-$ can be studied. One finds that the angular distribution of the produced W bosons is very forward peaked. That is, the W^- are produced preferentially along the direction of the incoming e^- in the CM system. This distribution is displayed, for two different beam energies, in Fig II.5. I shall not give here a detailed formula for $d\sigma/d\cos\theta$, as this expression is rather lengthy and can be found in the Yellow book[41].

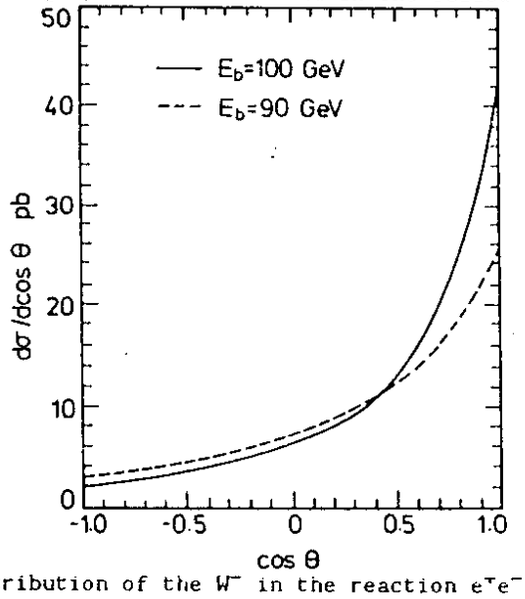

Fig II.5 Angular distribution of the W^- in the reaction $e^+e^- \to W^+W^-$. Here θ is the angle the W^- makes with respect to the incident e^- direction

One can understand the reason for the forward peaking shown in Fig II.5 rather easily. The ν exchange graph of fig II.1 contains a propagator proportional to the momentum transfer between the e^- and the W^-. This t^{-1} factor favors small angles between the e^- and the W^-.

A second qualitative feature which can also be easily understood refers to the helicity states of the produced W's. Precisely in the forward direction one of the produced W's must necessarily be longitudinally polarized, while the other is transversly polarized. Since longitudinally polarized W's arise only as a result of the W's having a mass, it is clear that the possibility of producing longitudinally polarized W's at LEP 200 is very interesting. Without the spontaneous breakdown of SU(2)xU(1), the W's would have been massless and only transversly polarized. Thus the longitudinally polarized W's are intimately connected with the mechanism of spontaneous breakdown. Unfortunately, as we shall see, away from the forward direction transversly polarized W's dominate and it is quite difficult to extract the purely longitudinally polarized component.

The fact that in the forward direction one has one longitudinal and one transverse W is a direct consequence of angular momentum conservation. The interactions that appear in Fig II.1 all involve vectorial vertices. Thus, neglecting the electron mass, it follows that the process $e^+e^- \to W^+W^-$ can only occur if the electron and positron have opposite helicities. The two relevant configurations leading to σ_{LR} and σ_{RL} are shown schematically in Fig II.6a. In the forward direction, it follows that the $W^+$and W^- helicities must add up to

unity and the relevant configurations are shown in Fig II.6b.

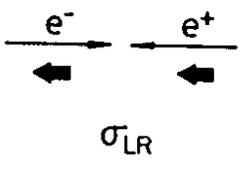

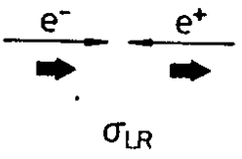

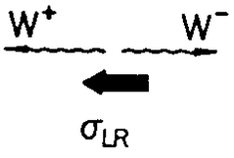

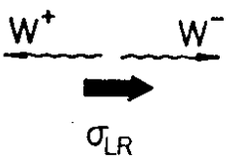

Fig II.6a Helicity configurations in the $e^+e^- \to W^+W^-$ scattering;

Fig II.6b W^+W^- helicities in the forward direction;

We see from this figure that, in the forward direction, for the case of σ_{LR} and σ_{RL} the allowed configurations are

$$\sigma_{LR} : \begin{cases} W^+(\lambda=1) & W^-(\lambda=0) \\ W^+(\lambda=0) & W^-(\lambda=-1) \end{cases} \qquad \text{(II.13a)}$$

$$\sigma_{RL} : \begin{cases} W^+(\lambda=-1) & W^-(\lambda=0) \\ W^+(\lambda=0) & W^-(\lambda=+1) \end{cases} \qquad \text{(II.13b)}$$

In fact, as we discuss below, σ_{LR} is very much greater than σ_{RL}, so that only the configurations given in Eq (II.13a) are relevant in the forward direction.

One can understand qualitatively why $\sigma_{LR} \gg \sigma_{RL}$ for $e^+e^- \to W^+W^-$, as follows. In Fig II.1, the neutrino exchange graph contributes only to σ_{LR}, because of the (V-A) form of the charged current interactions. The graphs involving the three gauge vertices contribute to both σ_{LR} and σ_{RL}, since they do not involve a purely (V-A) e^+e^- vertex. However, the σ_{RL} contribution is small because there exists a cancellation between the γ and the Z^0 graphs. In the limit in which one could neglect the Z^0 mass altogether, then instead of considering photon and Z^0 exchange, it would be equivalent to consider the exchange of W_3^μ and of Y^μ - the gauge boson coupled to the U(1) current. But only the W_3 gauge boson can couple to W^+W^- and it couples to e^+e^- in a (V-A) form. So in this limit, σ_{RL} actually vanishes! In fact, numerically, one finds $\sigma_{RL} \sim 10^{-2}\ \sigma_{LR}$, at the energies relevant for LEP 200[41].

Hagiwara et al[42] have studied in detail the fraction of W's produced at LEP 200 with a given polarization and a given production angle. Their results, which update and complement an earlier study of Gaemers and Gounaris[43] are displayed in Fig II.7.

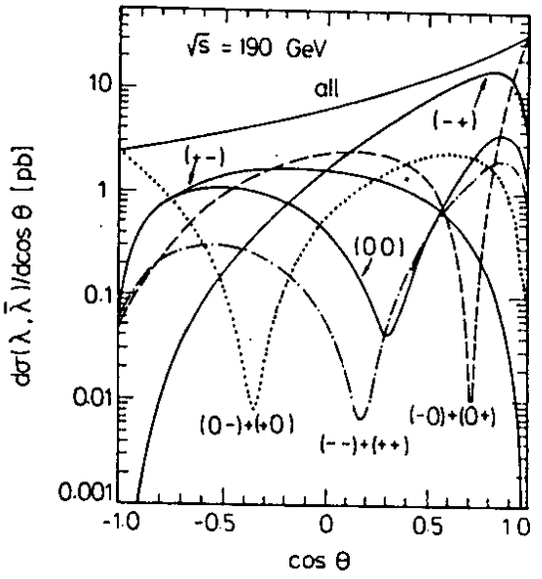

Fig II.7 Angular distribution for the process $e^+e^- \to W^+W^-$ at $\sqrt{s}$ = 190 GeV for different polarizations (λ_-, λ_+) of the produced W^- and W^+ bosons.

One notes from this figure that:
i) Apart from $\theta \approx 0$, where $W^-(-1)\ W^+(0)$ or $W^-(0)\ W^+(1)$ must dominate, by angular momentum conservation, the main polarization states produced are $W^-(-1)\ W^+(+1)$.
ii) The interesting $W_{Long.}\ W_{Long.}$ configuration (0,0) is not very relevant, except close to the forward direction. But even there it is a factor of five smaller than the transverse-transverse and transverse-longitudinal cross section.

In principle, one can try to separate out the various polarization contributions experimentally, by using the angular distribution of the produced fermions as a polarizaion analyzer. To do this, it is necessary to determine the direction of the W axis in the event. This is facilitated because, kinematically, the energy of the produced W must be that of the beam energy. Once this axis is determined, one can boost back the event to the W rest frame. In this frame, the angular distribution of the produced fermions (which materialize experimentally as jets if the fermions are quarks), depends on the W helicity. Let θ^* be the angle of a produced e^- (or d quark) with respect to the W^- axis in the W rest frame, as shown in Fig II.8. Then, because of the (V-A) form of the charged weak interactions, one finds the following angular distributions:

$$\frac{d_N}{d\cos\theta^*} \sim \begin{cases} \frac{1}{2}(1 + \cos\theta^*)^2 & \lambda = -1 \\ \sin^2\theta^* & \lambda = 0 \\ \frac{1}{2}(1 - \cos\theta^*)^2 & \lambda = +1 \end{cases} \qquad \text{(II.14)}$$

One can check these formulas qualitatively. For instance, since the $\bar{\nu}_e$ are right handed, at $\theta^* = 0$ it is clear that only a W^- of helicity -1 can contribute, as shown pictorially in Fig 9. This is precisely the result of Eq II.14.

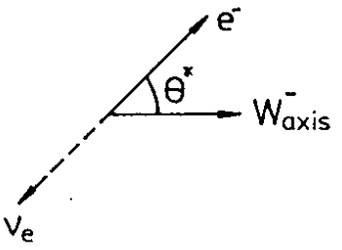

Fig II.8 Definition of the angle θ^*

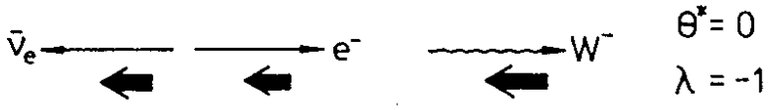

Fig II.9 Helicity considerations which show that only $W^-(-1)$ contributes for $\theta^* = 0$.

Obviously to be able to extract the angular distribution of W's of a given polarization, it is necessary to know the charge of the emitted fermion. For the case in which the W^+W^- pairs decay into 4 jets, this is not easily ascertained. Still one can distinguish between longitudinal and transversly polarized W's. Without charge identification one cannot tell the difference between $\lambda = \pm 1$, but both of these give rise to a transversly polarized W. So the angular distribution of jets in the W rest frame separates still W_{long} from W_{trans}. One has

$$\frac{dN}{d\cos\theta^*} \quad \begin{cases} \sin^2\theta^* & W_{long} \\ 1 + \cos^2\theta^* & W_{trans} \end{cases} \qquad (II.15)$$

where W_{trans} is the sum of the distribution for $\lambda = \pm 1$ in Eq II.14.

III. DETAILED W INVESTIGATIONS

One of the most interesting aspects of LEP 200 is the possibility to measure there the value of the W mass very precisely. As I discussed in Sec I, to test the electroweak radiative corrections it is necessary to measure accurately two out of the three quantities M_Z, $\sin^2\theta_W$ and M_W. As we have seen, a precise measurement of $\sin^2\theta_W$ at LEP 100 and the SLC is possible but difficult. Hence an accurate determination of M_W is very welcomed. This is particularly so in the case one were to find small deviations from the standard model at the Z^0, as there is no reason to believe that these deviations should affect the relationship between M_W and M_Z in the same way as they affect the relationship between $\sin^2\theta_W$ and M_Z.

From the fundamental formula relating M_W to Δr, Eq I.76, one readily computes the error in Δr as a function of possible errors in M_W and M_Z. One finds, approximately,

$$\delta\Delta r \approx \left[22 \left(\frac{\delta M_W}{M_W} \right)^2 + 43 \left(\frac{\delta M_Z}{M_Z} \right)^2 \right]^{1/2} \qquad (II.16)$$

The last term contribute an error to Δr of order $3\text{-}4\times10^{-3}$ if δM_Z can be kept, as expected,

below 50 Mev. One sees, therefore, that measuring M_W to ±100 MeV could push the error in Δr to

$$\delta\Delta r \lesssim 0.007 \qquad \text{(II.17)}$$

This clearly is an interesting goal for LEP 200. However, is it really possible to reduce the experimental error on M_W to the level of one part per mil?

This issue was investigated by Barbiellini et al[41], in the Yellow Report. They suggested four different methods for measuring M_W which involved:

i) Studying the threshold dependence of the $e^+e^- \to W^+W^-$ process

ii) Measuring the electron end point spectrum in the decay $W \to e\nu$

iii) Measuring the di-jet mass in the decay $W \to \bar{q}q'$

iv) Measuring the $e\nu$ invariant mass in the decay $W \to e\nu$

Each of these methods appears to be able to determine M_W with systematic and statistical errors in the 100-200 MeV range [(Process ii) is a little less precise[41]]. Because these methods are, in principle, independent, it is possible to combine their results. Thus a measurement of M_W with $\delta M_W \lesssim 100$ MeV appears to be feasible at LEP 200. I shall not discuss all the four methods to extract M_W in detail here, but I will make a few remarks on the threshold method and the jet-jet extraction of M_W. Both of these methods appear promising, but they will require a careful understanding of both theoretical and experimental subtleties.

Measuring M_W via the threshold dependence of $\sigma(e^+e^- \to W^+W^-)$ requires a scan and therefore some decision on how to optimize the running time per point. To get an idea of the statistical significance one could achieve, Barbiellini et al[41] considered the case shown in Fig II.10, in which 100pb^{-1} of data were taken distributed over 10 energies from E_b = 80 GeV to E_b = 100 GeV. This excercise leads to a statistical error on M_W of δM_W = 138 MeV. However, no attempt was made to really optimize this value.

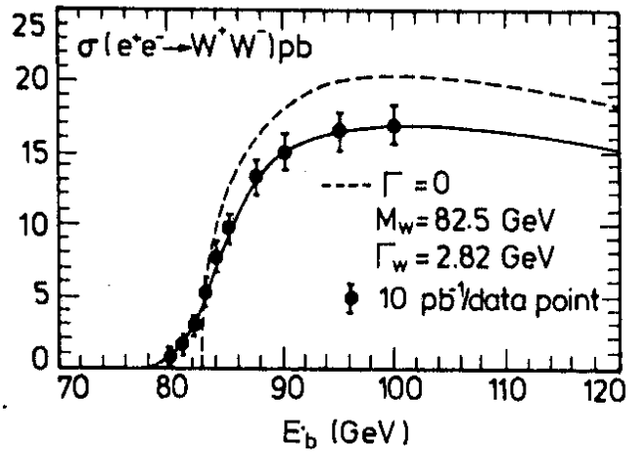

Fig II.10 Statistical errors and running time distribution leading to δM_W = 138 MeV, from Ref 41.

The calculations leading to Fig (II.10) incorporate two important effects not included in

the cross section plot of Fig II.3, namely the fact that the W's have a non zero width and that the final state W's are reconstructed from their decay byproducts. The finite W width makes the turn-on of the cross section less sharp than that of Fig II.3 and it is clearly an effect which must be included of one wants to extract M_W accurately. The fact that W events have to be reconstructed from the decay byproducts means that, in practice, events contribute to the cross section when their mass is $M_W \pm \Delta$. The graph in Fig II.10 uses a value of $\Delta = 10$ GeV, which contributes to depressing the value of the cross section beyond threshold. In addition, for a proper comparison, one really should use the radiatively corrected expressions for $\sigma(e^+e^- \to W^+W^-)$. Unfortunately, although electroweak radiative corrections for the process $e^+e^- \to W^+W^-$ have been computed [44], these results are not in a form which is particularly suited for experiments and probably will need to be partially redone. Provided these theoretical effects are incorporated, however, a value of M_W to $\delta M_W = \pm 100 - 200$ MeV seems clearly achievable with this method. The systematic error, as for the Z^0 case, is small, being only due to the beam energy calibration and should be able to to be kept well under 50 MeV.

Measuring the W-mass from the jet-jet invariant mass of its decay byproducts, at first sight, appears not to be very accurate because of calorimetric losses. If one reconstructs the 2 jets corresponding to each W in a 4 jet event by finding the W-axis, as shown schematically in Fig II.11, and imposes no additional constraint, then typically one finds an error $\delta M_W \simeq 2$ GeV. However, as suggested by Roudeau[45], the situation improves dramatically if one imposes as a constraint that the 2 jet energies should add up to E_{beam}, the beam energy. In this case, as shown in Fig II.12, the measured M_W in a Monte Carlo study differs from the input M_W by only $\delta M_W \simeq 80$ MeV. (The statistical error on this measurement is insignificant). This experimental "renormalization" seems to get rid of essentially all calorimetric losses!

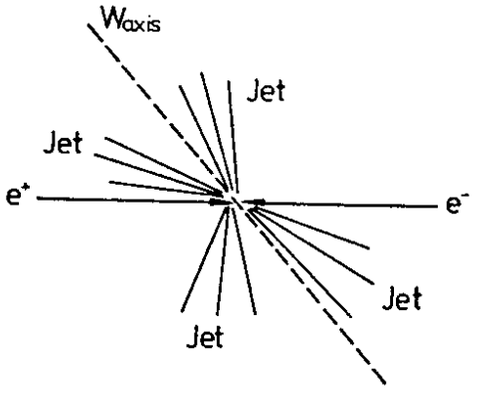

Fig II.11 Reconstructing W's from the process $e^+e^- \to W^+W^- \to 4$ jets

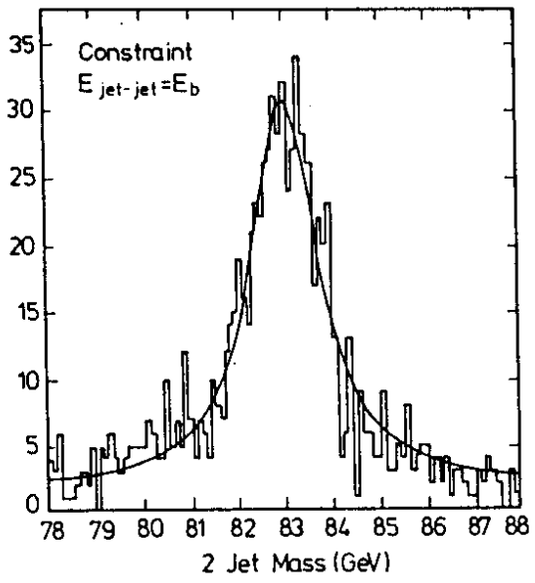

Fig II.12 Reconstructed 2 jet invariant mass with the constraint $E_{2\,jet} = E_b$. The input value was M_W = 83.2 GeV and the output value is M_W = 83.125 Gev. From Ref 41.

Although also this method looks very promising, one must worry about QED processes involving real photon emissions: $e^+e^- \to W^+W^-\gamma$, which will change the constraint $E_b = E_{2\,jet}$. One needs a separate correction for this effect, and it is not clear what errors it will induce on an M_W measurement. As one will know a value for M_Z very precisely at LEP 100 by other methods, it would be particularly important to try to test this new method for measuring mass with the hadronic decays of the Z^0. What value of M_Z will one get by imposing, in Z^0 hadronic decays, the constraint $E_{2\,jet} = 2E_b$? Perhaps a kinematically more closely akin test would involve measuring the Z^0 mass in the process $e^+e^- \to Z^0\gamma$, with the Z^0 decaying into hadrons and using the constraint $E_{2\,jet} = 2E_b - E_\gamma$. At any rate, these are tests which will allow one to better gauge the intrinsic accuracy of this method, which is peculiar of e^+e^- interactions, where the kinematics are fixed.

Besides the W mass, at LEP 200 one can study in some detail W decays, especially those into hadrons, which are difficult otherwise to study in hadronic machines. For quark decays, $W \to \bar{q}q'$, the branching ratio $B(W\to\bar{q}q')$ measures the appropriate element of the Kobayashi Maskawa matrix: $V_{qq'}$. As I mentioned earlier, if one neglects the effect of quark masses (more precisely, mass differences) the hadronic width into a given quark species is independent of $V_{qq'}$, since, by unitarity,

$$\sum_{q'} |V_{qq'}|^2 = 1 \qquad \text{(II.17)}$$

Apart from QCD corrections, this width is 3 times the width of the W into $l\bar{\nu}_e$:

$$\Gamma(W \to l\bar{\nu}_e) = \frac{G_F}{6\pi\sqrt{2}} M_W^3 \simeq 241 \text{ MeV} \qquad \text{(II.18)}$$

where the numerical value corresponds to M_W = 82 GeV. The effect of QCD corrections, as in the Z^0 case, is to multiply the hadronic branching ratio by $1+\frac{\alpha_s}{\pi}$. For the decay $W \to \bar{t}q'$ one needs, furthermore, to include the effects of the top mass, since this mass is non negligible. (Indeed $m_t > M_W$ is not excluded!)

The total rate $\Gamma(W \to \text{all})$ for the case of three generations can be written in terms of $\Gamma(W \to e\bar{\nu}_e)$ as

$$\frac{\Gamma(W \to \text{all})}{\Gamma(W \to e\bar{\nu}_e)} = \left\{ 3 + 3\left[2 + \left(1 + \frac{m_t^2}{2M_W^2}\right)\left(1 - \frac{m_t^2}{2M_W^2}\right)^2\right](1 + \frac{\alpha_s}{\pi}) \right\} \qquad \text{(II.19)}$$

Using m_t = 40 GeV and M_W = 82 GeV this formula leads numerically to $\Gamma_W \simeq 2.72$ GeV, which is quite near to the value expected for the total Z^0 width (c.f. Eq I.41). The individual hadronic ratios for decays not involving t quarks are given by

$$B(W \to \bar{q}q') = 3\,|V_{qq'}|^2(1 + \frac{\alpha_s}{\pi})\,B(W \to l\bar{\nu}_e) \simeq 0.277\,|V_{qq'}|^2 \qquad \text{(II.20)}$$

while for decays involving t-quarks one has

$$B(W \to \bar{t}q) = 3|V_{tq}|^2\,(1 + \frac{\alpha_s}{\pi})(1 + \frac{m_t^2}{2M_W^2})(1 - \frac{m_t^2}{M_W^2})^2\,B(W \to l\bar{\nu}_e)$$

$$\simeq 0.180\,|V_{tq}|^2 \qquad \text{(II.21)}$$

where the numerical values apply for m_t = 40 GeV, M_W = 82 GeV.

Depending on the flavor identification possibilities of the various LEP detectors, it should be possible, by studying hadronic W decays, to extract the value of some of the Kobayashi Maskawa matrix elements. Of particular interest is the value of V_{tb}. This is an element which actually can be readily singled out experimentally. The decay $W \to \bar{t}b$ will lead, in general, to multijet topologies with jets which are considerable softer than normal. These events, as shown in the Monte Carlo study of Fig II.13, have quite different characteristics than the usual W → jet-jet events. So a reasonable clean sample of $W \to \bar{t}b$ events can be selected, for example, by imposing a thrust cut of $T < 0.75$ and a jet multiplicity cut of $N_{jet} > 4$. Vertex detectors could in principle help to disentangle the contributions coming from $W \to \bar{t}b$ from those arising form $W \to \bar{t}s$ or $W \to \bar{t}d$. However, $|V_{tb}|^2$ is expected to be so much greater than $|V_{ts}|^2$ and $|V_{td}|^2$, from the unitarity of the Kobayashi Maskawa matrix. Thus essentially all W decays involving a t quark will also involve a b quark. So it is unlikely, therefore, that the handful of remaining events not involving a b quark can be unambiguously separated.

It is clear that with 500 pb^{-1} of data one will have a very interesting sample of W hadronic decays to analyze. Even with only 30% efficiency to detect hadronic decays of the W's, one would be left with over 4000 such decays to study. Although this is a small sample in comparison to many other "weak decay" experiments, it is a theoretically very clean sample to study weak intentions involving hadrons. In contrast to charm decays, for example,

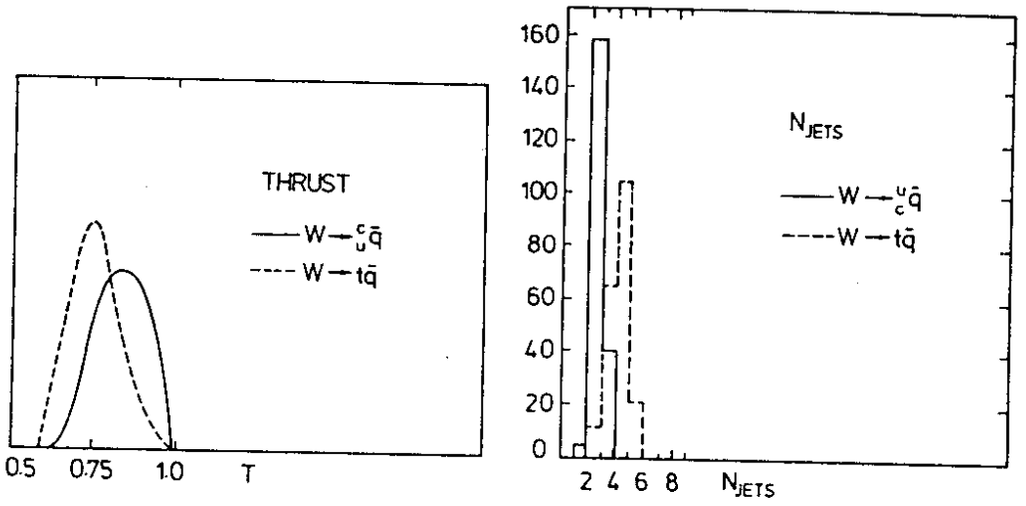

Fig II.13 Difference in thrust and number of jets in $W \to \bar{t}q$ decays compared to other W hadronic decays. From Ref 41

where the QCD effects are many and difficult to disentangle because the q^2 is small, in W decays these effects should be manageable. This difference is displayed pictorially in Fig II.14.

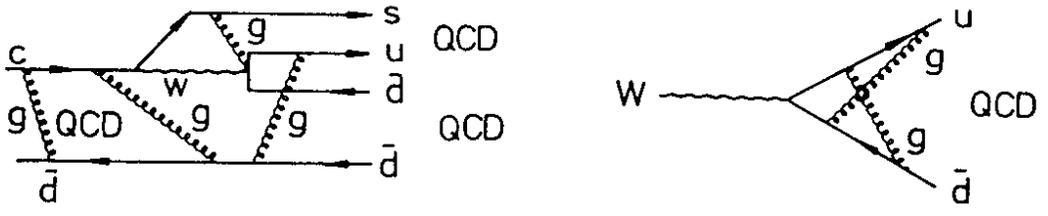

Fig II.14 QCD effects in weak decays of a D-meson and in the decay of the W.

There are many other detailed studies that can be performed at LEP 200 involving W production. I shall return to an example of such a study, involving properties of the 3 gauge vertex, at the end of these lectures.

III HIGGS SEARCHES AT LEP

One of the most interesting issues to be pursued at the SLC and at LEP is the search for Higgs bosons in the available energy range. Before discussing the various methods to look for Higgses in e^+e^- interactions, I want to recall first some general properties of Higgs bosons in the standard model.

IIIa GENERAL FEATURES OF THE HIGGS SECTOR IN THE STANDARD MODEL

In the electroweak model of Glashow Salam and Weinberg[1] the breakdown of SU(2) x U(1) to $U(1)_{em}$ is effected by an SU(2) doublet field which is complex. Thus this field

$$\Phi = \begin{pmatrix} \phi^0 \\ \phi^- \end{pmatrix} \tag{III.1}$$

describes in toto, four excitations. The breakdown is caused by assuming that Φ has asymmetric self interactions, governed by a potential

$$V(\Phi) = \lambda(\Phi^+\Phi^- - \frac{1}{2} v^2)^2 \tag{III.2}$$

This potential forces Φ to obtain a non trivial vacuum expectation value

$$\langle\Phi\rangle = \frac{1}{\sqrt{2}} \begin{pmatrix} v \\ 0 \end{pmatrix} \tag{III.3}$$

which leads then to the desired breakdown: $SU(2) \times U(1) \rightarrow U(1)_{em}$. Because of this breakdown, of the 4 real fields in Φ, 3 get eaten by the $W^{\pm}$ and Z^0 gauge bosons, to provide these fields with mass. However, one neutral field in Φ remains as a physical excitation. This is the Higgs boson H. In models where the breakdown mechanism is more complicated, as in supersymmetric models where more than one doublet of Higgs is involved, more physical excitations remain in the theory. However, in the standard model, the only physical remnant of the symmetry breakdown is the Higgs boson H. Clearly its detection would be of fundamental importance.

The $W^{\pm}$ and Z^0 masses arise form the gauge invariant kinetic energy term for the doublet Φ:

$$\mathcal{L} = -(D_\mu\Phi)^+ (D^\mu\Phi) \tag{III.4}$$

where the covariant derivative D_μ, since Φ has hypercharge -1/2, reads

$$D_\mu\Phi = (\partial_\mu - ig \frac{\tau_i}{2} W_{\mu i} + ig' \frac{1}{2} Y_\mu)\Phi \tag{III.5}$$

Here g and g' are SU(2) and U(1) coupling constants, which in lowest order, are related to the electromagnetic charge via Eq (I.58). It is easy to see that the vacuum expectation value (III.3) generates a mass for the charged $W^{\pm}$ fields and the combination of neutral fields $gW_3^\mu - g'Y^\mu$, which is proportional to the Z^0 field. Using the relationship between W_3^μ and Y^μ, and Z^μ and A^μ, characterized by the Weinberg angle,

$$\begin{pmatrix} W_3 \\ Y \end{pmatrix} = \begin{pmatrix} \cos\theta_W & \sin\theta_W \\ -\sin\theta_W & \cos\theta_W \end{pmatrix} \begin{pmatrix} Z \\ A \end{pmatrix} \tag{III.6}$$

and Eq (I.58), one has

$$gW_3^\mu - g'Y^\mu = (g/\cos\theta_W)Z^\mu \tag{III.7}$$

Hence it is easy to see that the $W^{\pm}$ and Z^0 masses are given by

$$M_W = \frac{1}{2} gv \quad ; \quad M_Z = \frac{1}{2} \frac{gv}{\cos\theta_W} \tag{III.8}$$

which shows the characteristic interrelation between M_W and M_Z, due to doublet breaking. From Eq (III.8) and Eq (I.18) one identifies, to lowest order, the Fermi scale v as

$$v = (\sqrt{2}\, G_F)^{-1/2} \approx 250 \text{ GeV} \tag{III.9}$$

From Eq (III.4) one can extract the coupling of the Z and W bosons to the physical Higgs boson. For this purpose, it is convenient to parametrize Φ in a way in which the fields which are eventually absorbed by the W and Z bosons are explicitly separated out as an overall phase factor. This is accomplished by writing Φ as

$$\Phi = \frac{e}{\sqrt{2}}\, e^{\,i\,\frac{\vec{\xi}\cdot\vec{\tau}}{v}} \begin{pmatrix} v+H \\ 0 \end{pmatrix} \tag{III.10}$$

Obviously the triplet of fields $\vec{\xi}$ does not contribute to $V(\Phi)$. Furthermore, it is also rather easy to show that $\vec{\xi}$ can be removed from Eq (III.4), via and SU(2) gauge transformation. So for our purposes, one can just use effectively

$$\Phi \equiv \frac{1}{\sqrt{2}} \begin{pmatrix} v+H \\ 0 \end{pmatrix} \tag{III.11}$$

with H being the physical Higgs field. Using the above in Eq (III.4), along with the mass relationships (III.8), yields the following trilinear Higgs-gauge couplings

$$\mathcal{L}_{H-g} = -\frac{e}{\sin 2\theta_W} M_Z Z^\mu Z_\mu H - \frac{e}{\sin\theta_W} M_W W_+^\mu W_{-\mu} H \tag{III.12}$$

Note that the Higgs coupling is proportional to the mass of the particle it couples to. This is a characteristic property of the Higgs boson, which also applies to its coupling to fermions.

The doublet Higgs Φ can couple to the quarks and leptons via SU(2) x U(1) invariant Yukawa couplings. If i and j are family indices, the most general form for these couplings is given by

$$\mathcal{L}_{Yukawa} = -\Gamma^u_{ij} (\bar{u}_i \bar{d}_i)_L \Phi\, u_{jR} + \Gamma^d_{ij} (\bar{u}_i \bar{d}_i)_L \tilde{\Phi}\, d_{jR} + \Gamma^l_{ij} (\bar{\nu}_{l_i} l_i)_L \tilde{\Phi}\, l_{jR} + \text{h.c.} \tag{III.13}$$

where

$$\tilde{\Phi} = i\tau_2 \Phi^* \tag{III.14}$$

When Φ is replaced by Eq (III.11), the vacuum expectation value v will give rise to mass matrices for the quarks and leptons of a given charge

$$M^f_{ij} = \frac{1}{\sqrt{2}} \Gamma^f_{ij} v \qquad f = \{ u, d, l \} \tag{III.15}$$

To go to a physical basis, these mass matrices must be diagonalized by (bi) unitary transformations on the fermion fields. (These transformations are the one which result in the appearance of the Kobayashi Maskawa matrix for the charged weak current). Since, however, ν is always accompanied by H, these transformations also diagonalize the fermion Higgs couplings, so that the resulting Higgs-fermion Lagrangian is just

$$\mathcal{L}_{H-f} = -m_f \bar{f}f - \frac{m_f}{v} \bar{f}fH \qquad \text{(III.16)}$$

for each species of fermions f. Again, these couplings are proportional to mass.

The Higgs boson mass is easily worked out from the Higgs potential (III.2). One finds

$$M_H^2 = 2\lambda v^2 \qquad \text{(III.17)}$$

Unfortunately since the parameter λ is unknown, the value of the Higgs mass is undetermined in the standard model. Thus searches for Higgs bosons, in as wide a mass range as possible, are very interesting. As we shall see, with LEP one can hope to produce Higgs bosons with measurable rates if their mass is less than about 100 GeV. (The direct process $e^+e^- \to H$ can produce Higgses with $M_H = 2E_b$, but because of the tiny coupling of H to e^+e^- pairs, this direct production is not experimentally observable). Higgses of mass less than 100 GeV are kinematically forbidden to decay into either W or Z pairs. In view if Eq (III.16) any Higgs boson produced at LEP, therefore, will decay into the heaviest fermion anti-fermion pair which is kinematically allowed. If $M_H < 2m_t$, these will be a $b\bar{b}$ pair. Otherwise the dominant Higgs decay is into $t\bar{t}$ pairs. A simple calculation gives for the Higgs boson width into a fermion and and antifermion the expression

$$\Gamma(H \to f\bar{f}) = \frac{G_F m_f^2}{4\sqrt{2}\,\pi} M_H \beta^3 \begin{pmatrix} 3 \\ 1 \end{pmatrix} \qquad \text{(III.18)}$$

where the upper factor above applies for quarks and the lower factor for leptons. Here $\beta = (1 - 4m_f^2/M_H^2)^{1/2}$. This width is very narrow. For instance, if $m_t > 30$ GeV, a 60 GeV Higgs will decay dominantly into $b\bar{b}$ pairs with a width of order 3 MeV!

IIIb HIGGS SEARCHES AT THE Z^0

Since at LEP and the SLC one will have of order 10^6 Z^0 per year one can look for the Higgs in Z^0 decays, even though the relevant branching ratios are not very large. The best Z^0 decay channels for searching for Higgses appear to be $Z^0 \to Hl\bar{l}$ and $Z^0 \to H\nu\bar{\nu}$[46]. Both of these reactions make use of the Z^0Z^0H coupling of Eq III.12 to produce the Higgs, as depicted in Fig III.1.

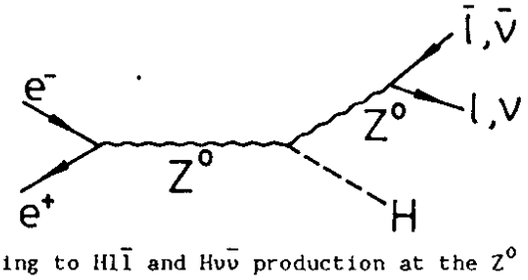

Fig III.1 Diagram contributing to $Hl\bar{l}$ and $H\nu\bar{\nu}$ production at the Z^0 pole.

The differential decay width for the dilepton process was calculated long ago by Bjorken[47], who obtained

$$\frac{d\Gamma(Z^0 \to Hl\bar{l})}{dx} = \frac{\alpha}{\pi \sin^2 2\theta_W} \frac{[1 - x + x^2/12 + 2z^2/3]\,[x^2 - 4z^2]^{1/2}}{[x - z^2]^2} \qquad \text{(III.19)}$$

Here $x = 2E_H/M_Z$ and $z = M_H/M_Z$, with the kinematic range for x being given by

$$2z < x < 1 + z^2 \qquad \text{(III.20)}$$

Because of the Z^0 propagator factor, the differential rate (III.19) favors the production of lepton paris with as large an invariant mass as possible. One has

$$m_{l\bar{l}} = M_Z(1 + z^2 - x)^{1/2} \quad \to \quad M_Z - M_H \qquad \text{(III.21)}$$

Fig III.2 displays this peaking behaviour, which constitutes a characteristic signature for the decay $Z^0 \to Hl\bar{l}$. This is a useful handle to have, since the total branching ratio for this

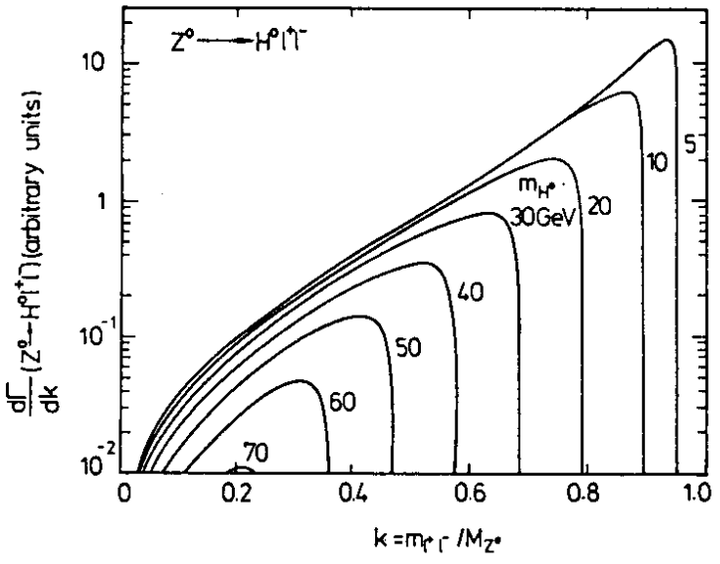

Fig III.2 Dilepton mass distribution for the process $Z^0 \to H\, e^+e^-$ for various Higgs masses. From Ref 46

process drops rather rapidly as a function of the Higgs mass, as illustrated in Fig III.3, taken from the Yellow Report[46]. For $M_H \sim 40$ GeV, one is left with just a handful of events of the type Hl^+l^- for every million Z^0's!

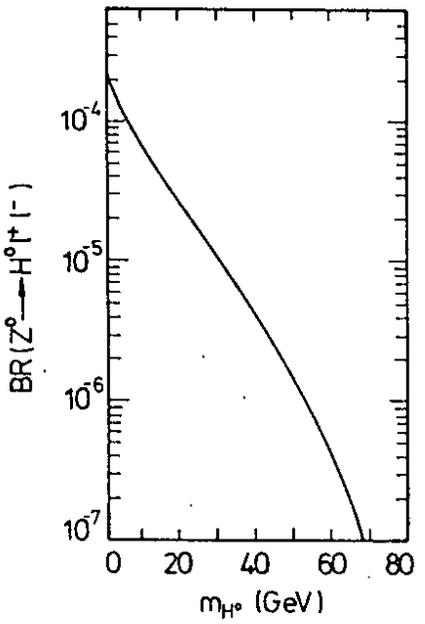

Fig III.3 Branching ratio for the process $Z^0 \rightarrow Hl\bar{l}$ as a function of the Higgs mass, from Ref 46

Under these circumstances one has to evaluate very carefully the effects of possible backgrounds. This matter was studied by H. Baer et al[46], who concluded that the background processes are in fact manageable by applying cuts which reduce the signal less than a factor of 2. The principal source of background, if it is kinematically allowed, is provided by the decay of a Z^0 into $t\bar{t}$ which then produces 2 jets and a l^+l^- pair. This background can be tamed by imposing a missing energy cut of $E_{miss} < 15$ GeV and requiring that the produced leptons be energetic and isolated ($E_{l_1} > 15$ GeV, $E_{l_2} > 5$ GeV). The result of this calculation, including also the $b\bar{b}$ background, is shown in Fig III.4.

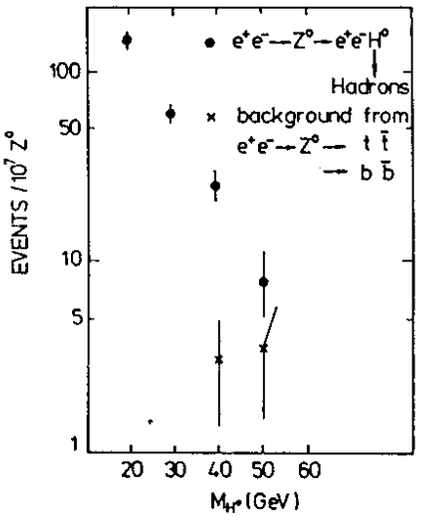

Fig III.4 Event rate (for 10^7 Z^0's!) and background level arising from $Z^0 \rightarrow t\bar{t} + b\bar{b}$ from the MC calculation of Ref 46.

The process $Z^0 \to H\nu\bar{\nu}$ is also quite interesting for a Higgs search, since the branching ratio for this process is about 6 times greater than that for $Z^0 \to Hl\bar{l}$ (c.f. Eq I.20). The signal is, however, less distinctive than in the lepton pair case, since there are more sources of background which can produce two jets plus missing energy. Baer et al[46], at any rate, have also studied this channel and conclude that it can be dug out of the background, with appropriate cuts, if M_H = 20 GeV; but Higgs detection becomes problematic if M_H is above 30 GeV. In any event, for processes with such low rates, like the production of Higgses from the Z^0, it is very useful to have more than one channel to look for a signal!

IIIc HIGGS SEARCHES IN TOPONIUM DECAYS

Despite the early indications of UA$_1$[5] of a top signal with 30 GeV < m_t < 50 GeV, nobody really knows for sure if the t quark is that light. However, it is certainly a reasonable possibility that the associate $t\bar{t}$ bound states, toponium, will be in the range of LEP 100 and the SLC. (Toponium physics, however, will be difficult, if not impossible, at the SLC because of the larger energy spread of the e^+e^- beams there). If this is the case, then one can foresee that, besides Z^0 physics, a very active program of investigation connected with toponium, will take place. Three aspects of toponium are particularly interesting to study. They concern:

i) The $t\bar{t}$ spectrum itself

ii) The weak interaction properties of t quarks

iii) Higgs production from toponium

Although the third point will be the main focus of my discussion here, let me make a few brief remarks on the other two points.

Toponium spectroscopy is, in principle, very rich. For the ψ system one has two states below open charm threshold, while for the Υ system one has three states below open bottom threshold. For toponium, on the other hand, one can estimate[48] that there will be, approximately, $2(m_t/m_c)^{1/2}$ states below the continuum limit. So of order 10 states for $m_{t\bar{t}} \sim 80$ GeV! However, most of these $t\bar{t}$ states will not be accessible because of the worsening of the energy spread, as one goes to higher energies. The energy spread at LEP is expected to be[49]

$$\delta E_{LEP} \simeq [4.4 \times 10^{-3} s(GeV^2)] \text{ MeV} \qquad \text{(III.22)}$$

Since for a narrow J=1 $t\bar{t}$ resonance

$$\int d\sqrt{s}\, \sigma(e^+e^- \to l^+l^-) = 6\pi^2 \frac{\Gamma^2(t\bar{t} \to l^+l^-)}{M^2_{t\bar{t}}\, \Gamma_{tot}(t\bar{t})} \qquad \text{(III.23)}$$

one can estimate the signal expected, from a knowledge of the toponium width into lepton pairs and the magnitude of this branching ratio. Although these quantities depend in detail on the quarkonium potential, a reasonable estimate[10] is that

$$\Gamma\left((t\bar{t})_{1S} \to l^+l^-\right) \simeq 5 \text{ KeV} \qquad \text{(III.24)}$$

with a branching ratio of order 10%. With these numbers and the LEP energy spread, it is easy to check that the $(t\bar{t})_{1S}$ signal for $M_{t\bar{t}} \sim 70$-80 GeV is about twice the background arising from non resonant $e^+e^- \to l^+l^-$, due to photon and Z exchange:

$$\int_{\text{Resonance Region}} \sqrt{s}\, d\sigma\,(e^+e^- \to l^+l^-) = (\delta E)_{LEP}\ \sigma(e^+e^- \to l^+l^-)\Big|_{\sqrt{s}=M_{t\bar{t}}} \qquad \text{(III.25)}$$

Things get rapidly worse for excited toponium states because the leptonic widths decrease. Nevertheless, it should be pointed out that the signal itself is not small. If $M_{t\bar{t}} \sim 70$-80 GeV the total rate into toponium is of the order of 100 pb or 30 events a day at the LEP nominal luminosity.

If top is in the LEP 100 energy range, one of the interesting questions to study is the spectrum of the lowest toponium bound states. Both the splitting between the 2s and 1s states and the leptonic width of the 1s triplet state are sensitive to the Coulombic part of the interquark potential. These quantities, therefore, depend on the value of the QCD Λ-parameter, which governs the evolution of the strong coupling constant. This dependence, for the case of the leptonic width, is displayed in Fig III.5 and, as can be seen, the differences are significant, especially for larger values of $M_{t\bar{t}}$.

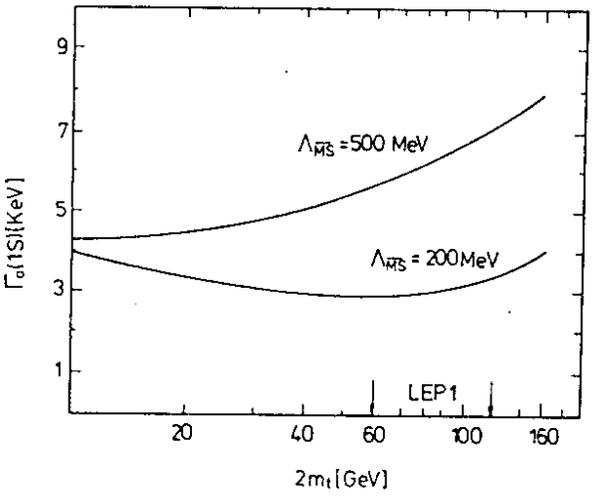

Fig III.5 Dependence of $\Gamma(1s \to l\bar{l})$ on $\Lambda_{\overline{MS}}$. From Ref 10

Although toponium is in many ways analogous to the charm and bottom quarkonia, there is a very important difference, connected with the weak interaction properties of the top quark. In contrast to the case of the ψ and Υ states, it is no longer true that the decay $(t\bar{t}) \to$ 3 gluons is the dominant mode of deexcitation of toponium. There are two reasons for this:
i) As the $(t\bar{t})$ states get nearer in mass to the Z^0, the decay of toponium will be dominated by the production of a virtual Z^0, which then decays into fermion antifermion pairs.
ii) The t quark, in the $(t\bar{t})$ bound state, will weak decay into a b quark and a virtual W. This single quark decay (SQD) rate grows as $(m_t)^5$ and thus becomes dominant for heavy toponia.

The various branching fractions of toponium, as a function of $2m_t$, are displayed in Fig III.6, where the above trends are clearly seen. The two body channels dominate at the Z^0 peak, while the SQD rises rapidly and is the most important branching ratio beyond $2m_t \simeq$ 70 GeV, except at the Z^0 peak.

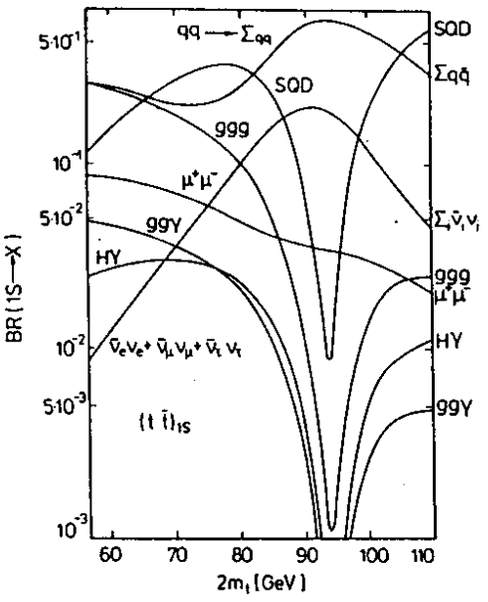

Fig III.6 Branching ratio of the triplet $(t\bar{t})_{1S}$ state, as a function of $2m_t$. From Ref 10

The presence of a dominant SQD above $2m_t \simeq 70$ GeV means that toponium decays will give rise to multijet events, which provide a good signature for the existence of toponium experimentally. If $m_t \lesssim \frac{1}{2} M_Z$, as we discussed in Sec I, one will know m_t to within a couple of GeV and so one can localize toponium rather easily. For $m_t > M_Z$, the presence of toponium will give rise to abundant spherical events. Again these will serve to identify the toponium location, especially if one makes topological cuts on the data. Of course if m_t is much greater than M_W, the rate for the process $t \to bW$ will be so fast that the $t\bar{t}$ state itself will cease to exist, since there will not be enough time for the quarkonium to form! At any rate, the SQD width is independent of the Kobayashi Maskawa matrix, because of the unitarity of this matrix. One finds

$$\Gamma(t\bar{t})_{SQD} \simeq \frac{G_F^2 m_t^5}{192\pi^3} \left(18 \sum_q |V_{tq}|^2\right) \simeq \frac{3G_F^2 m_t^5}{32\pi^3} \qquad \text{(III.26)}$$

neglecting small phase space corrections.

Probably the most interesting aspect of toponium is related to the search for Higgses. The decay of $(t\bar{t})$ into $H\gamma$ has a substantial branching ratio for toponium in the LEP energy range. One can compute the ratio of $(t\bar{t})$ into $H\gamma$, compared to the toponium leptonic rate, rather precisely, since the wavefunction at the origin cancels in the ratio. From the diagrams of Fig III.7 one easily calculates[50]

$$R = \frac{\Gamma((t\bar{t}) \to H\gamma)}{\Gamma((t\bar{t}) \to l^+l^-)} = \frac{G_F M^2_{t\bar{t}}}{4\pi\sqrt{2}\alpha} \left(1 - \frac{M^2_H}{M^2_{t\bar{t}}}\right) \qquad \text{(III.27)}$$

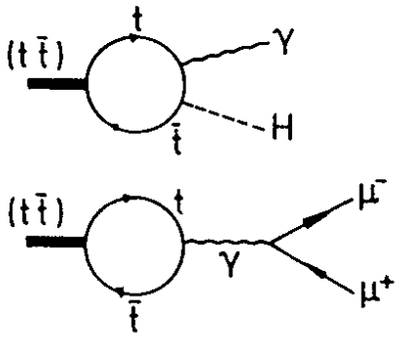

Fig III.7 Diagrams contributing to toponium decay into Hγ and l^+l^-

This rate, actually, has rather large QCD corrections, which have been computed by Vysotski[51]. For $M_{t\bar{t}}$ of order M_W, R ≈ 1/2. Thus the Hγ branching ratio is non negligible, being of order 5% (see Fig III.6) for Higgses not too near the kinematical limit. Given the rate of production of toponium, one sees that, for M_H ≈ 40 GeV, the process $(t\bar{t}) \to H\gamma$ gives rise to a few Higgs events a day. This is to be contrasted with the few event a year expected from the decay $Z^0 \to Hl^+l^-$, for Higgses of the same mass!

Buchmüller et al[10], in the Yellow report, have estimated the integrated luminosity needed to detect Higgs bosons of a given mass in toponium decays. Because the decay $(t\bar{t}) \to H\gamma$ has a very clear signature, consisting of an energetic γ produced opposite to a dijet, one can hope to detect Higgs bosons with masses up to $M_{t\bar{t}} - 10$ GeV, if $m_t < \frac{1}{2} M_Z$. For heavier toponia, the situation is slightly less favorable because the γ plus dijet background is worse. Fig III.8 give the integrated luminosity needed to detect a 3σ Higgs effect in toponium decay, for different values of $M_{t\bar{t}}$. As can be seen in Fig III.9, for a "light" toponium the signal stands out clearly from the γ+jets background, almost all the way to the kinematical limit.

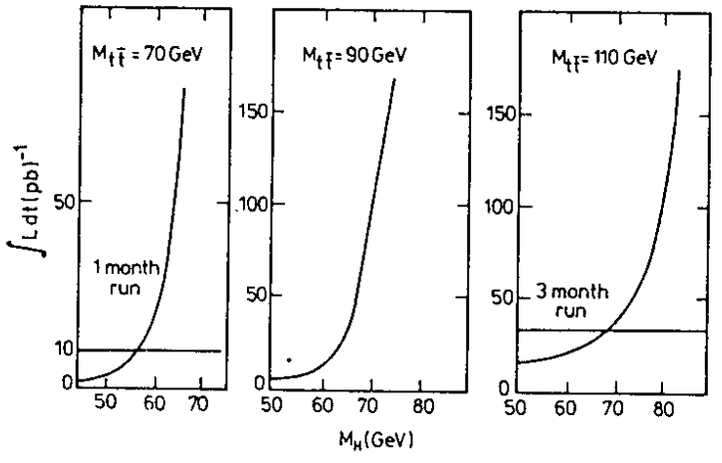

Fig III.8 Integrated luminosity needed to detect a 3σ Higgs signal in $(t\bar{t}) \to H\gamma$. From Ref 10

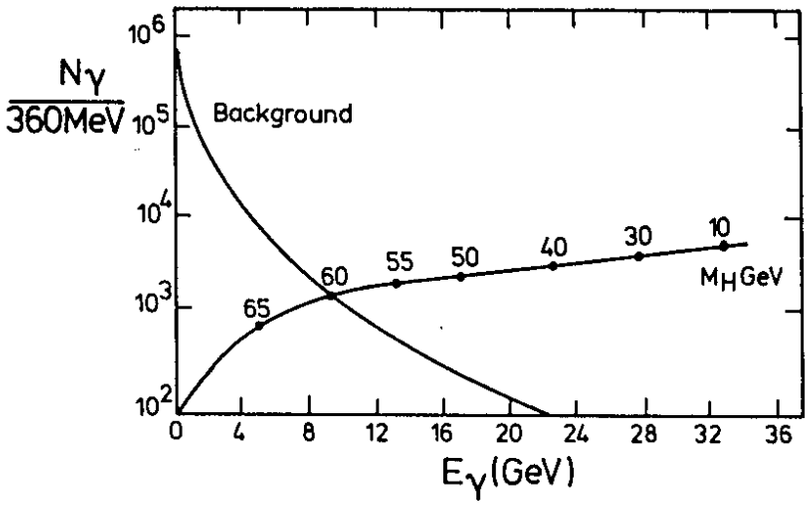

Fig III.9 Signal and background for the decay $(t\bar{t}) \to H\gamma$, for different M_H and $M_{t\bar{t}} = 70$ GeV. From Ref 10.

It should be clear from these figures that, if toponium is in the range of LEP 100, the process $(t\bar{t}) \to H\gamma$ is the best way to search for Higgses of mass above 10 GeV.

IIId HIGGS SEARCHES BEYOND THE Z^0

It could be that the Higgs mass is above that of toponium, or top itself is very massive, so that no Higgs signal is seen at LEP 100 or the SLC. This could easily happen, say, if $M_H \gtrsim 60$ GeV. In these circumstances LEP 200 can provide a further window for a Higgs search up to masses nearing $M_H \approx 100$ GeV. Above the Z^0 energy range, the most effective means of producing Higgses is in associated production with Z^0's. The diagram is the same as that studied at the Z^0 pole (Fig III.1), except that now the produced Z^0 is real and not virtual. The cross section for the process $e^+e^- \to Z^0H$ has been calculated by a number of authors[52], with a particularly complete set of formulas being given by Kelly and Shimada, who also considered the subsequent decay of the Z^0 into lepton pairs. One finds

$$\sigma(e^+e^- \to Z^0H) = \frac{\pi\alpha^2[1+(1-4\sin^2\theta_W)^2]P(P^2+3M^2_Z)}{24\sin^4\theta_W\cos^4\theta_W(s-M_Z^2)^2\sqrt{s}} \qquad \text{(III.28)}$$

where P is the 3-momentum of the Z^0:

$$P = \frac{1}{2}\left[\, s - 2M_Z^2 - 2M_H^2 + \frac{1}{s}(M_Z^2 - M_H^2)^2 \,\right]^{1/2} \qquad \text{(III.29)}$$

This cross section is plotted for various values of the Higgs mass in Fig III.10

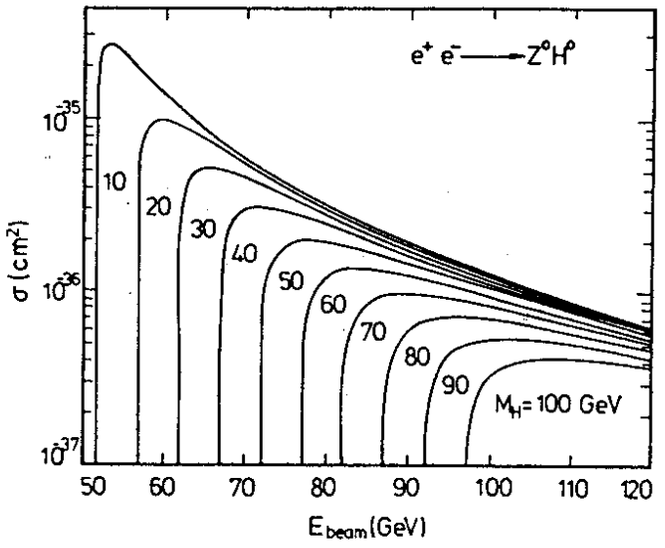

Fig III.10 Total cross section for the process $e^+e^- \to HZ^0$, as a junction of M_H and the beam energy

One can see from Fig III.10 that:

i) the cross section for $e^+e^- \to HZ^0$ is not too strongly energy dependent after the threshold rise

ii) the cross section itself is smallish ($\sigma \lesssim 1$ pb for $M_H \gtrsim 50$ GeV) but is measurable at LEP 200 where one hopes to be able to collect 500 pb^{-1} of data per year. For reference, remember $\sigma(e^+e^- \to W^+W^-) \sim 20$ pb.

Of course, to actually measure this cross section one must identify the Z^0 and so one really ends up by reducing the number of events, since not all Z^0 decays lead to easily identifiable signals. The techniques to use are again very similar to those employed for the Higgs search at the Z^0 pole. The cleanest signal is provided by the decays of the Z^0 into lepton pairs, leading to processes with 2 jets back to back to an l^+l^- pair. A less distinctive signal is provided by the $Z^0 \to \nu\bar{\nu}$ decay, although this rate is six times greater than that into l^+l^-. The most favorable process, from the point of view of rate, would use the hadronic decays of the Z^0. However, the ensuing 4 jet process is difficult to separate from other 4 jet backgrounds, like W^+W^- production into 4 jets.

H. Baer et al[46] did a Monte Carlo analysis of the process $e^+e^- \to HZ^0$, with the Z^0 decaying into lepton pairs and into neutrino pairs for $\sqrt{s}$ = 160 GeV and for M_H = 50 GeV. As can be seen from Figs III.11 and III.12, the signal appears to be detectable above background in both cases.

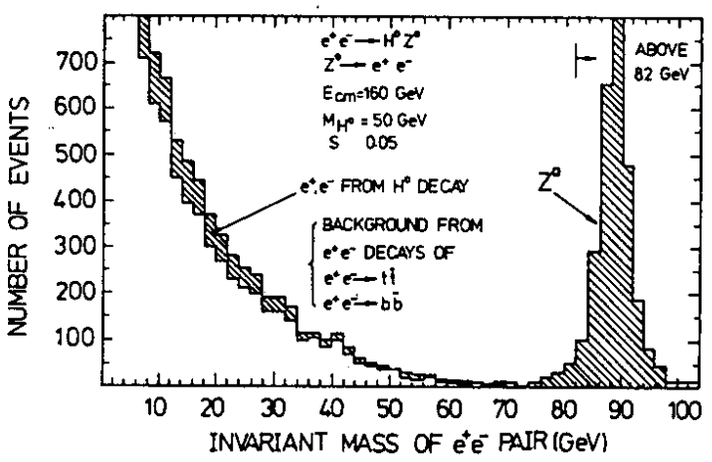

Fig III.11 MC analysis of the e^+e^- invariant mass distribution from $e^+e^- \to H+(Z^0 \to e^+e^-)$, compared to backgrounds from $e^+e^- \to t\bar{t}$ and $b\bar{b}$. From Ref 46

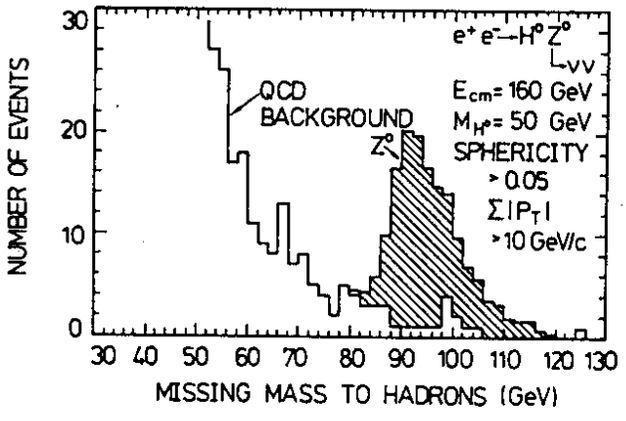

Fig III.12 MC analysis of the $e^+e^- \to H^0+(Z^0 \to \nu\bar{\nu})$ process, showing the missing mass recoiling against the observed hadrons. From Ref 46

To give an example at higher energies, at $\sqrt{s}$ = 180 GeV, with an integrated luminosity of 500 pb^{-1}, one expects for M_H = 80 GeV about 350 events of HZ^0 associated production. Since $B(Z^0 \to \mu^+\mu^-) \simeq 3\%$, this means approximately 10 events/year of the type 2 jets back to back to a $\mu^+\mu^-$ pair and about 60 events of the type 2 jets with unbalanced missing energy, corresponding to the $Z^0 \to \nu\bar{\nu}$ decays. These are very small number of events, but fortunately so is the background. However, above $\sqrt{s} > 2M_Z$ one has to worry about the Z^0Z^0 background, which to be eliminated requires very good recoil mass resolution[41]. My conclusion is that at LEP 200 one will be able to find Higgses up to masses of order 80-90 GeV, but it will require a very dedicated effort.

IIIe NON CONVENTIONAL HIGGSES

All the above discussion assumed that the breakdown of $SU(2)xU(1)_{em}$ to $U(1)_{em}$ was effected by one doublet Higgs field ϕ. Actually, all the neutral current phenomenology which provides the most stringent tests of the standard model is not affected if there is more than one Higgs doublet, since the ratio of NC to CC interactions remains the same. Obviously, however, the Higgs sector physics is radically altered if there is more than one Higgs doublet. Consider specifically the case of two Higgs doublets ϕ_1 and ϕ_2. These represent 8 real fields. When the ϕ_i acquire vacuum expectation value, the Higgs mechanism takes place and 3 fields are absorbed to give mass to the W^+, W^- and Z^0 gauge bosons. Thus one is left over with 5 physical excitations: three neutral fields, H_0, H_0' and H_0'', and two charged fields, H^+ and H^-. These latter excitations are the most characteristic signal of having more than one Higgs doublet, and since they are charged they can be pair produced via the electromagnetic interactions. (They couple also to the Z^0).

I want to discuss a little more the doublet case, because it is of some theoretical importance being what is expected in supersymmetric extensions of the standard model[53]. It may not be immediately obvious why supersymmetry demands a doubling of Higgses, but one can see this in two different ways:

i) A supersymmetric extension of the standard model should not spoil the renormalizability of the model. This appears to be a trivial requirement, since supersymmetry just associates fermionic excitations to bosonic ones, and viceversa[53]. However, unless one doubles the number of Higgs doublets in the theory, it is no longer true that all Adler Bell Jackiw chiral anomalies[54] for the gauge currents vanish. This vanishing of the Adler Bell Jackiw anomalies is satisfied if the sum of the charges of all fermions in the theory vanishes[55]

$$\sum_i Q_i = 0 \qquad \text{(III.30)}$$

Then the triangle graphs of Fig III.13, involving the gauge currents, can be easily checked to be non anomalous. Only if this is so will the renormalizability of the standard model not be jeopardized, for the presence of these anomalies spoils the proof of renormalizability[55].

Fig III.13 Triangle graph leading to an ABJ anomaly, unless Eq(III.30) is satisfied

Eq(III.30) is satisfied if the sum is over the charges of the quarks and leptons. It is not satisfied if we supersymmetrize the theory with only one Higgs doublet, since its fermionic partner, the Shiggs, has charges

$$\phi_f = \begin{pmatrix} \psi^0 \\ \psi^- \end{pmatrix} \qquad \text{(III.31)}$$

Only by having two Higgs doublets, of opposite hypercharge

$$\Phi_1 = \begin{pmatrix} \phi_1^0 \\ \phi_1^- \end{pmatrix} \quad ; \quad \Phi_2 = \begin{pmatrix} \phi_2^+ \\ \phi_2^0 \end{pmatrix} \tag{III.32}$$

will one be able to trivially supersymmetrize the theory, without running into troubles with Eq(III.30) and renormalizability.

ii) Supersymmetry attaches scalars to fermions of a given helicity. In non supersymmetric models, one can write the Yukawa interactions involving up- and down-like quarks by using both Φ and its charge conjugate $\tilde{\Phi} = i\tau_2 \Phi^*$ (c.f. Eq III.13). However, taking complex conjugation changes the helicity properties and it is not possible to couple fermions to both Φ and Φ^* in a supersymmetric way. Thus if one wants to give masses to both the charge $\frac{2}{3}$ quarks and the charge $-\frac{1}{3}$ quarks via Yukawa interactions, it is necessary to have two distinct fields fields Φ_1 and Φ_2. Φ alone allows only one kind of coupling to take place, without violating supersymmetry.

As I mentioned earlier, if there are charged Higgs bosons, as one expects in a two Higgs doublet situation, they will be pair produced in e^+e^- interactions. Thus, if their mass is low enough, they will be detectable at the SLC and LEP. The γ and Z^0 exchange graphs of Fig (III.14) are readily computed. The coupling of the Z^0 to H^+H^- is the standard one, arising through the neutral current interaction of Eq I.6. One has

$$\mathcal{L}_{int} = \frac{e}{\cos\theta_W \sin\theta_W} (J_3^\mu - \sin^2\theta_W J_{em}^\mu) Z_\mu$$

$$= e\cot 2\theta_W [H^- \partial^\mu H^+ - H^+ \partial^\mu H^-] Z_\mu \tag{III.33}$$

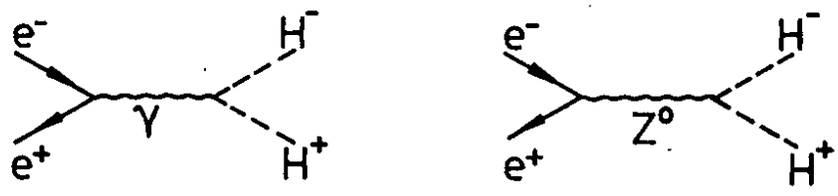

Fig III.14 Graphs contributing to $e^+e^- \to H^+H^-$

The cross section for this process is shown in Fig III.15, for various values of the charged Higgs mass. Two points should be remarked upon. The cross section turns on rather slowly, due to a β^3 threshold factor which is characteristic of the p-wave production of scalar particles. Furthermore, the cross section itself is a factor of 1/4 smaller compared to that for producing vector-like fermion-antifermion pairs (i.e. fermions with $A_f = 0$). These circumstances will make the detection of charged Higgses not easy. The most distinguishing characteristic of H^+H^- production is that the angular distribution of the H^+ with respect to the e^+ incoming direction will be proportional to $\sin^2\theta$, rather than the usual $1 + \cos^2\theta$ of fermions. This may not be enough of a handle, though, given the smallish rate.

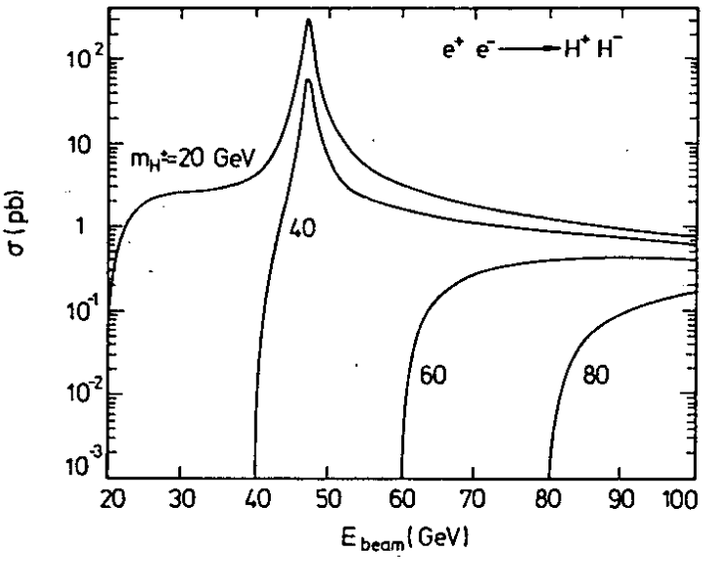

Fig III.15 Cross section for $e^+e^- \to H^+H^-$, for various values of M_{H^+}. From Ref 46

As a final comment, I note that if M_{H^+} is light enough for the process $t \to bH^+$ to be kinematically allowed, then this decay totally dominates over the normal weak decay of top. This is clear since the Higgs decay rate is proportional to $G_F\, m_t^3$, while the ordinary t weak decay is proportional to $G_F^2\, m_t^5$. Indeed the rate $t \to bH^+$ is so fast, that toponium would disintegrate before it had a chance to form! So the observation of toponium itself will provide an indirect bound for M_{H^+}: $M_{H^+} \gtrsim m_t - m_b$.

IV NONSTANDARD PHYSICS AT LEP

Up to now I have considered, for the most part, only the expectations of the standard model[1] at LEPenergies. It could well be that at the SLC and at LEP one will find deviations from the standard dogma. Indeed this is one of the exciting aspects, and one of the benefits, of exploring a new energy regime! One can imagine three ways in which deviations from standard expectations may crop up:

i) The experimental results which are supposed to provide precision tests of the standard model will not agree with the expected theoretical results. For example, $\Delta r \neq 0.07$ or $\Gamma_{tot}(Z^0)$ will differ from the value predicted by the standard model.

ii) New channels are seen, producing particles which do not belong to the standard model menagerie.

iii) Predicted cross sections show deviations from expectations. For instance, the total or differential cross section for $e^+e^- \to W^+W^-$ may not quite be those expected in the Glashow Salam Weinberg model[1].

Of course, a single new phenomena can give contributions to more than one of the above categories.

In the last part of my lectures, I want to briefly discuss some possibilities for "new physics" which might be seen at LEP and the SLC. My discussion will not be very extensive and

the interested reader is referred to the Yellow Report, where many other theoretical speculations are discussed, especially in the reports of H. Baer et al[46] and G. Barbiellini et al[41].

IVa GENERAL FORMULA

If the novel phenomena, which is presumed to appear in the LEP energy range, has to do with the production of new particles, one needs to have an estimate of the size of the production cross section. If these new particles have electroweak couplings, then their pair production rate is readily obtained, given their SU(2)xU(1) assignments, by the computation of the usual graphs, involving photon and Z^0 exchange. As many of the exotic phenomena suggested fall in this category (e.g. further generations of quarks and leptons, supersymmetric partners of known excitations, excited electrons or muons, etc), it is worthwhile giving a general formula for the pair production cross section as a function of the SU(2)xU(1) quantum numbers of the "new stuff". I shall detail this first for the case of fermion pair production. Let T_{3L} and T_{3R} be the weak isospin of the left and right handed components of the fermions, respectively, and let Q be their charge in units of e. Then one finds[56]:

$$\sigma_f(Q,T_{3L},T_{3R},\beta,s) = \frac{4\pi\alpha^2}{s}\,\beta\,\frac{(3-\beta^2)}{2}\cdot\Big\{ Q^2 - \frac{-2QC_VC'_Vs(s-M_Z^2)}{(s-M_Z^2)^2+M_Z^2\Gamma_Z^2} +$$

$$+ \frac{(C_V^2+C_A^2)s^2}{(s-M_Z^2)^2+M_Z^2\Gamma_Z^2}\cdot\Big[C_V'^2+C_A'^2\,\frac{2\beta^2}{3-\beta^2}\Big]\Big\} \qquad \text{(IV.1)}$$

In the above C'_V and C'_A are related to the vector and axial couplings of the produced fermions

$$C'_A = \frac{-2(T_{3L}+T_{3R}) + 4Q\sin^2\theta_W}{4\sin\theta_W\cos\theta_W} \qquad \text{(IV.2a)}$$

$$C'_A = \frac{2(T_{3L}-T_{3R})}{4\sin\theta_W\cos\theta_W} \qquad \text{(IV.2b)}$$

while C_V and C_A are the corresponding couplings for the electrons. That is $C_V = C'_V$, $C_A = C'_A$ for $Q = -1$, $T_{3L} = -1/2$ and $T_{3R} = 0$. The parameter β is the usual threshold factor

$$\beta = (1 - 4m_f^2/s)^{1/2} \qquad \text{(IV.3)}$$

and one sees that σ_f is proportional to β, except for the $C_A'^2$ term. The β^3 dependence of this term arises because the axial current can only generate the fermions in a p-wave[46].

One can readily obtain a similar formula for pair producing scalars of weak isospin T_3 and of charge Q, with the result[56]:

$$\sigma_s(Q, T_3, \beta, s) = \frac{1}{4}\beta^3 \sigma_f(Q, T_3, T_3, 1, s) \qquad \text{(IV.4)}$$

This cross section has a β^3 threshold factor because it is pure p wave and it is down by factor of 1/4 from the corresponding (vector-like) fermion formula, as I already remarked when I discussed H^+H^- production. Note also that for scalars the C_A' term vanishes. Armed whith these formulas, it is quite easy to discuss a variety of processes. In what follows, I shall concentrate on the production of supersymmetric partners of quarks and leptons, so that Eq (IV.4) is the relevant equation.

IV SOME ASPECTS OF SUPERSYMMETRY AT LEP

Supersymmetry associates bosonic with fermionic excitations and vice versa, keeping the number of degrees of freedom of the bosons and fermions the same[53]. Two supersymmetric multiplets are relevant when one considers a supersymmetric extension of the standard model. The (1, 1/2) multiplets of gauge fields and their associated gauginos and the (1/2, 0) multiplets of quarks and leptons with their associated scalar excitations, the squarks and the sleptons. Note that to each spin 1/2 fermion, supersymmetry assigns a complex scalar excitation, since the degrees of freedom must match.

The interactions of the superpartners, in the supersymmetric extension of the standard model, are fixed by supersymmetry. However, the masses of the superpartners themselves are assumed arbitrary, since supersymmetry must be broken to be realistic. (Exact supersymmetry would predict $m_{fermion} = m_{boson}$, and is obviously not tenable experimentally). It is easy to write down the interactions implied by supersymmetry. Effectively one just substitutes pairwise two particle terms with two sparticle terms. This is shown pictorially in Fig IV.1, for the vertex which couples a Z^0 to a fermion antifermion pair. Supersymmetry generates vertices in which the Z^0 couples to the scalar partners of the fermions as well as gaugino sfermion fermion vertices.

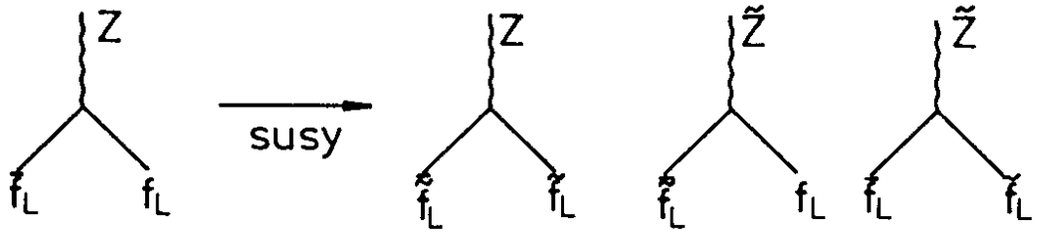

Fig IV.1 Vertices generated by supersymmetry. The fields with a tilde are superpartners.

Note that one associates different scalars to the left and right handed fermions ($f_L \to \tilde{f}_L$; $f_R \to \tilde{f}_R$, where the tilde denotes a superpartner). Gauge fields, as shown in Fig IV.1, couple to scalar partners of the same handedness.

Using Eq(IV.4) one can easily compute the pair production of squarks and sleptons. The

results for squarks of mass $m_{\tilde{q}}$ = 40 GeV are shown in Fig IV.2. Note that the cross sections are different, depending on the type of squark one is producing: $\tilde{u}_L$, $\tilde{u}_R$, $\tilde{d}_L$ or $\tilde{d}_R$. This is easy to understand, at the Z^0, since the cross section is the proportional to $C_V^{'2}$ and thus is different for the various squarks. Unfortunately Fig (IV.2) is too optimistic, as squarks with mass as low as 40 GeV are already excluded by the UA1 analysis of their monojet sample[57]. Indeed the present limits for squarks lie in the range of $m_{\tilde{q}} \gtrsim$ 60-80 GeV, so that direct squark production could only be relevant for LEP 200.

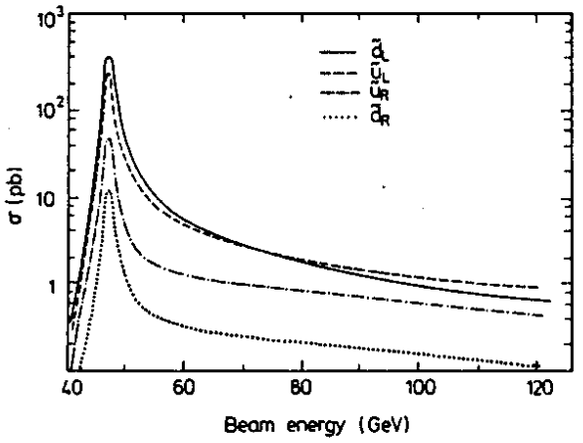

Fig IV.2 Production of squarks of $m_{\tilde{q}}$ = 40 GeV, which illustrates the difference in rate for different species. From Ref 46.

Similar graphs can be obtained for sleptons. An example, taken from Ref 46, is shown in Fig IV.3, in which one considers the production of selectrons of various masses. In this case, besides the photon and Z^0 exchange graphs, one must also consider t-channel graphs involving gaugino exchange. These graphs, an example of which is shown in Fig IV. 4, can produce two selectrons of different handedness, in contrast to the gauge exchange graphs. The bottom curves in Fig IV.3 correspond to the production of selectrons of different handedness. These cross sections are clearly much smaller.

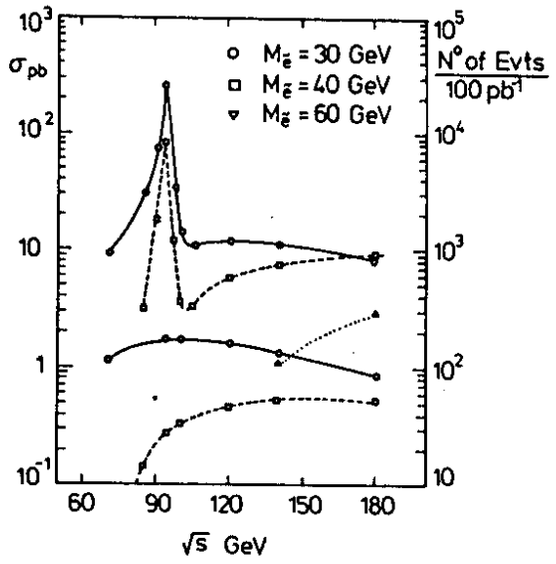

Fig IV.3: Selectron production at LEP, for different selectron masses. The top curves

correspond to the sum of $\tilde{e}_R^+\tilde{e}_R^-$ and $\tilde{e}_L^+\tilde{e}_L^-$, while the bottom curves give the cross section for selectrons of opposite handedness. From Ref 46.

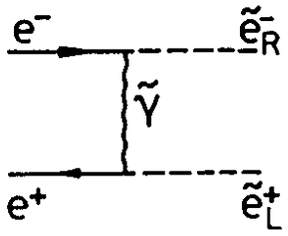

Fig IV.4: Graph which contributes to the production of selectrons of opposite handedness.

Also Fig IV.3 may be too optimistic, as selectrons have rather strong bounds, for light photinos. These bounds arise from a study both at SLAC and at DESY of the process $e^+e^- \to \gamma\tilde{\gamma}\tilde{\gamma}$, with the photinos leaving the apparatus. The results shown in Fig IV.5, suggest that, for selectrons, masses below 50 GeV may be unrealistic. So also here, LEP 200 appears to be needed for a SUSY search.

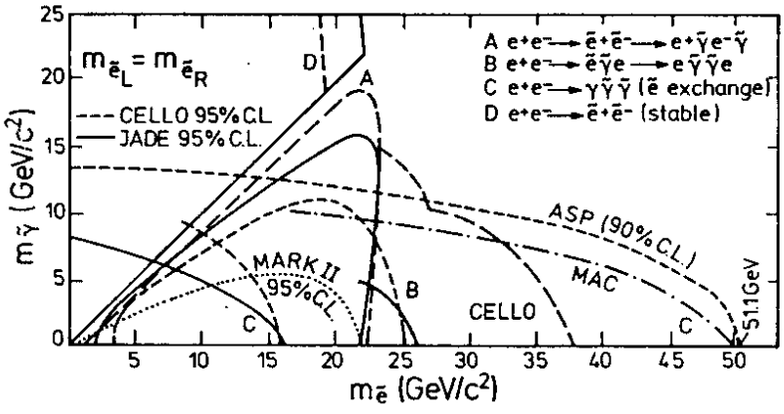

Fig IV.5: Bounds on selectrons from the process $e^+e^- \to \gamma\tilde{\gamma}\tilde{\gamma}$, from Ref 61.

If, and when, supersymmetric particles are produced at LEP, their signals will be rather distinctive, so that their detection may be possible even for rather low rates. Since all vertices contain always two supersymmetric particles, sparticles must always decay into another sparticle and an ordinary particle. In particular, the lightest supersymmetric particle (LSP) is stable. This LSP is though to be the photino, for a variety of theoretical arguments[58]. Since the photino interacts rather weakly, it will leave the detector, leading to events with an energy imbalance. So if supersymmetric particles exist in the LEP range, they will manifest themselves in events with missing energy. Thus it is important to have as hermetic a detector as possible. One must also worry about backgrounds which could be misinterpreted as a supersymmetric signal. For example, since a typical chain for selectron decay is $\tilde{e} \to e\tilde{\gamma}$, the process $e^+e^- \to \tilde{e}^+\tilde{e}^-$ will give rise to events containing an acollinear pair, plus missing energy. These sort of events could be faked by ordinary $\tau^+\tau^-$ production, with a subsequent electronic decay of both τ's. Fortunately this background can be eliminated with appropriate angle and energy cuts on the produced leptons[46]. This suppression of backgrounds also works for other SUSY channels, as is discussed in the report of H. Baer et

al[46]. Thus one concludes that a SUSY signal will be detected at LEP, provided it is there!

IVc TESTING THE THREE GAUGE VERTEX

As a last topic, let me discuss briefly how one may be able to look for possible deviations in the 3 gauge vertex at LEP 200. Such deviations may arise, for example, if the W bosons were not themselves elementary. Although this possibility is probably farfetched, it is not totally out of the question[59] and certainly ought to be tested, as well as possible, experimentally.

The γW^+W^- and $Z^0W^+W^-$ vertices are given in the standard model by Eq II.5 and II.6. If one had no prejudices, except for Lorentz invariance, one would describe these vertices by seven distinct form factors[43], for each vertex. Imposing P, C and T conservation reduces these numbers to three[43]. In the static limit, where one neglects all possible q^2 dependence of the form factors, these form factors reduce to 3 parameters: an overall coupling, which plays the role of the charge, and a magnetic moment and a quadrupole moment term. For the standard model, of course, the value of the magnetic moment and of the quadrupole moment is fixed. For physical $W^{\pm}$, where terms proportional to the gauge particle momentum are dropped if they are to be contracted with the polarization tensor ($\epsilon^{\alpha}(q)\ q_{\alpha}=0$), one can write, in general, the 3 gauge vertex as[42)43)]

$$\Gamma_V^{\mu\alpha\beta}(P, q, \bar{q}) = ig_{VWW}\Big\{ (\bar{q}-q)^{\mu}\left[\left(1+\frac{\lambda_V P^2}{2M_W^2}\right)\eta^{\alpha\beta} - \frac{\lambda_V P^{\alpha}P^{\beta}}{M_W^2}\right] + \\ + (P^{\alpha}\eta^{\mu\beta} - P^{\beta}\eta^{\mu\alpha})\,[1+\kappa_V+\lambda_V]\Big\} \qquad \text{(IV.5)}$$

The parameter κ_V and λ_V are related to the magnetic moment and the quadrupole moment by[60]

$$\mu_V = \frac{e}{2M_W}(1+\kappa_V+\lambda_V)$$

$$Q_V = -\frac{e}{M^2_W}(\kappa_V-\lambda_V) \qquad \text{(IV.6)}$$

In the standard model $\lambda_V = 0$ and $\kappa_V = 1$, as can be easily checked.

Values of κ_V and λ_V different from the expectations of the standard model will change the differential angular distribution for the process $e^+e^- \to W^+W^-$. An example of the changes is given in Fig IV.6, for the case in which $\lambda_V = 0$, $\kappa_\gamma = 1$ but κ_Z is allowed to vary. Clearly the changes shown in the above figure are not very big and it is interesting to ask what is the minimum value for which one can expect that deviations will be measurable. This was studied by means of a Monte Carlo simulation by Barbiellini et al[41], for the case in which $\kappa_\gamma = \kappa_Z = \kappa$ and $\lambda_V = 0$. These authors concluded that with 500 pb^{-1} of data, one could restrict κ to lie within ±10% of unity. A later study by Hagiwara et al[42] considered also

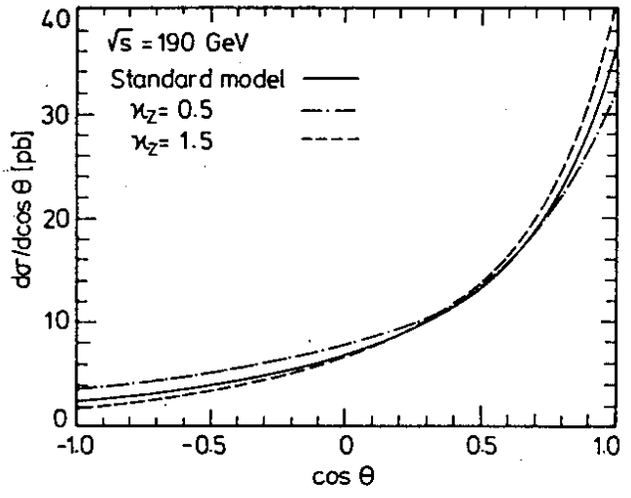

Fig IV.6: Differential cross section for $e^+e^- \to W^+W^-$ for two different values of κ_Z.

static parameters which violate P, C and T, and examined more complicated experimental correlations. They also concluded that κ can be measured to ±10% at LEP 200 and that, in fact, the angular distribution of the produced W's was the best parameter to measure, if one wanted to bound CP conserving static parameters in the 3 gauge vertices. Because an accurate measurement of this angular distribution needs the identification of the W charge, experimentally one is restricted to study W^+W^- process producing 2 jets plus and $l\nu_l$ pair. This effectively reduces the number of useful events by a factor of 2. So to get a 10% measurement of κ will be very challenging.

ACKNOWLEDGEMENTS

The very nice atmosphere provided in Sandhamn by A. Caton, P.O. Hulth. and C. Jarlskog, combined with the enthusiasm of the students at the school, made the giving of these lectures a very enjoyable task. Part of these lectures were also given at the XIV International Winter Meeting on Fundamental Physics in St. Feliu de Guixols and I would like to thank A. Mendez and A.J. Grifols for their hospitality there.

REFERENCES

1) S.L. Glashow, Nucl. Phys. 22 (1961) 579;
S. Weinberg, Phys. Rev. Lett. 19 (1967) 1264;
A. Salam in Elementary Particle Theory, ed. N. Svartholm
(Almquist and Wiksell, Stockholm 1968);

2) N. Cabbibo, Phys. Rev. Lett. 10 (1963) 531;
M. Kobayashi and K. Maskawa, Prog. Theo. Phys. 49 (1973) 652;

3) T. Appelquist and H. Georgi, Phys. Rev. D8 (1973) 4000;

A. Zee, Phys. Rev. D8 (1973) 4038;

4) G. Altarelli, YR I 3;

5) G. Arnison et al, Phys. Lett. 147B (1984) 493;

6) S. Güsken, J.H. Kühn and P.M Zerwas, Phys. Lett. 155B (1985) 185;

7) See for example, J. Schwinger Particle Sources and Fields, Vol II, (Addison Wesley, Reading, Mass 1973) p. 397;

8) V. Novikov et al, Phys. Rept. C41 (1978) 1;

9) F.M. Renard, Z. Phys. C1 (1979) 225;
J.H. Kühn and P.M. Zerwas, Phys. Lett. 154B (1985) 448;
P.J. Franzini and F.J. Gilman, Phys. Rev. D32 (1985) 237;
L.J. Hall, S.F. King and S.R. Sharpe, Nucl. Phys. B260 (1985) 510;
S. Güsken, J.H. Kühn and P.M. Zerwas, Nucl Phys. B262 (1985) 393;
A. Martin, Phys. Lett. 156B (1985) 411; see also
W. Buchmüller et al, YR I 203;

10) W. Buchmüller et al, YR I 203;

11) M. Consoli, S. Lo Presti and L. Maiani, Nucl. Phys. B223 (1983) 474;

12) R. Kleiss, YR I 153;

13) A. Blondel et al, YR I 35;

14) G. Barbiellini, B. Richter and J.L. Siegrist, Phys. Lett. 106B (1981) 414;
E. Ma and J. Okada, Phys. Rev. Lett. 41 (1978) 287;

15) K.J.F. Gaemers, R. Gastmans and F.M. Renard, Phys. Rev. D19 (1979) 1605;

16) E. Simopoulou, YR I 197,

17) M. Caffo, R. Gatto and E. Remiddi, Phys. Lett. 173B (1986) 91; UGVA-DPT 1986/09-514;

18) C. Maña and M. Martinez, DESY 86-062, Nucl. Phys. B to be published;

19) J. Bartels, A. Fridman, T.T. Wu and A. Schwarz; Z. für Phys. C23 (1984) 295;

20) A. Sirlin, Phys. Rev. D22 (1980) 971;

21) L. di Lella, Proceedings of 1985 International Symposion on Lepton and Photon Interactions at High Energy, Kyoto Japan 1985, ed. by M. Konuma and R. Takahashi; (Nissha printing Co, Kyoto 1986)

22) W. Marciano and A. Sirlin, Phys. Rev. D22 (1980) 2695; Nucl. Phys. B189 (1981) 442,

23) C. Llewellyn Smith and J. Wheater, Phys. Lett. 105B (1981) 486; Nucl. Phys. B208 (1982) 27 and B226 (1983) 547 (E)

24) J. Kim et al, Rev. Mod. Phys. 53 (1980) 211;

25) J. Panman in Proceedings of the 12th International Conference on Neutrino Physics and Astrophysics, Sendai Japan, 1986;

26) H. Abramowicz et al, Phys. Rev. Lett. 57 (1986) 298;

27) W. Marciano and A. Sirlin, Phys. Rev. D22 (1980) 2695 and D29 (1984) 945; M. Consoli, S. Lo Presti and L. Maiani, Ref 11; Z. Hioki, Prog. Theo. Phys. 68 (1982) 2134; Nucl. Phys. B229 (1983) 284;

28) A. Sirlin, Phys. Rev. D29 (1984) 89;

29) Review of Particle Properties, Phys. Lett. 170B (1986) 1;

30) W. Marciano, Phys. Rev. D20 (1979) 274;

31) B.W. Lynn and R.G. Stuart, Nucl. Phys. B253 (1985) 216;

32) W. Wetzel, Nucl. Phys. B227 (1983) 1;

33) M. Consoli and A. Sirlin, YR I 63;

34) P. Baillon et al, YR I 172;

35) B.W. Lynn, M. Peskin and R.G. Stuart, YR I 90;

36) M. Greco, YR I 82;

37) J. Chaveau, YR I 177;

38) W. Wetzel, Z. für Phys. C11 (1981) 117;

39) O.P. Sushkov, V.V. Flambaum and I.B. Khriplovich, Sov. J. Nucl. Phys. 20 (1975) 537;

40) W. Alles, Ch. Boyer and A.J. Buras, Nucl. Phys. B119 (1977) 125;

41) G. Barbiellini et al, YR II 1;

42) K. Hagiwara, R.D. Peccei, D. Zeppenfeld and K. Hikasa, Nucl. Phys. B282 (1987) 253;

43) K.J. Gaemers and G.J. Gounaris, Z. für Phys. C1 (1979) 259;

44) M. Lemoine and M. Veltman, Nucl. Phys. B164 (1980) 445; R. Philippe, Phys. Rev. D26 (1982) 1588;

45) P. Roudeau, YR II 73; see also G. Barbiellini et al, Ref 41;

46) H. Baer et al, YR I 297;

47) J.D. Bjorken, Proceedings of the 1976 SLAC Summer Institute on Particle Physics, ed. M.C. Zipf (SLAC-198, 1977);

48) C. Quigg and J.L. Rosner, Phys. Lett. 72B (1978) 462;

49) J.M. Jowett, preprint CERN LEP TH 85-04;

50) F. Wilczek, Phys. Rev. Lett. 39 (1977) 1304;

51) M.I. Vysotsky, Phys. Lett. 97B (1980) 159;

52) B.L. Ioffe and V.A. Khoze, Sov. J. Part. Nucl. 9 (1978) 50; B.W. Lee, C. Quigg and H.B. Thacker, Phys. Rev. D16 (1977) 1519; R.L. Kelly and T. Shimada, Phys. Rev. D23 (1981) 1940;

53) For a review see for example H.E. Haber and G.L. Kane, Phys. Rep. 117C (1985) 75;

54) S. Adler, Phys. Rev. 177 (1969) 2426; J.S. Bell and R. Jackiw, Nuovo Cimento 60A (1969) 49;

55) D.J. Gross and R. Jackiw, Phys. Rev. D6 (1972) 477; C. Bouchiat, J. Iliopoulos and P. Meyer, Phys. Lett. 38B (1972) 519;

56) N. Deshpande, X. Tata and D. Dicus, Phys. Rev. D29 (1984) 1527;

57) A. Homma, Proceedings of the XXIII International Conference of High Energy Physics, Berkeley, Calif., July 1986;

58) J. Ellis, J.S. Hagelin, D.V. Nanopolous, K.A. Olive and M. Srednicki, Nucl. Phys. B238 (1984) 453;

59) For a recent review, see B. Schrempp., Proceedings of the XXIII International Conference of High Energy Physics, Berkeley, Calif., July 1986;

60) K.J. Kim and Y.-S. Tsai, Phys. Rev. D7 (1973) 3710;

61) Compilation due to W. de Boer;